HHS Public Access

Author manuscript

Small. Author manuscript; available in PMC 2019 December 27.

Published in final edited form as:

Small. ; : e1801183. doi:10.1002/smll.201801183.

Multifunctional electrospun nanofibers for enhancing localized cancer treatment

Yike Fu,

State Key Laboratory of Silicon Materials, School of Materials Science and Engineering, Zhejiang University, Hangzhou, 310027, P.R. China.

Dr. Xiang Li,

State Key Laboratory of Silicon Materials, School of Materials Science and Engineering, Zhejiang University, Hangzhou, 310027, P.R. China., xiang.li@zju.edu.cn

Dr. Zhaohui Ren,

State Key Laboratory of Silicon Materials, School of Materials Science and Engineering, Zhejiang University, Hangzhou, 310027, P.R. China., hgr@zju.edu.cn

Prof. Chuanbin Mao, and

Department of Chemistry & Biochemistry, Stephenson Life Sciences Research Center, University of Oklahoma, 101 Stephenson Parkway, Norman, Oklahoma, 73019-5300, USA., cbmao@ou.edu

Prof. Gaorong Han

State Key Laboratory of Silicon Materials, School of Materials Science and Engineering, Zhejiang University, Hangzhou, 310027, P.R. China.

Abstract

Localized cancer treatment is one of effective strategies in clinical destruction of solid tumors at the early stage as it can minimize the side effects of the cancer therapeutics. Electrospun nanofibers have been demonstrated as a promising implantable platform in localized cancer treatment, enabling the on-site delivery of therapeutic components and the minimal side effect to normal tissues. This review discusses the recent cutting-edge research with regard to electrospun nanofibers used for various therapeutic approaches, including gene therapy, chemotherapy, photodynamic therapy, thermal therapy, and combination therapy, in enhancing the localized cancer treatment. Further, it extensively analyzes the current challenges and potential breakthroughs in utilizing this novel platform for clinical transition in localized cancer treatment.

Keywords

electrospun nanofibers; localized drug delivery; localized cancer treatment; cancer therapeutics

Electrospun nanofibers has gained much attention as a promising treatment for solid tumors due to the on-site drug delivery and low side effect. This review presents an overview of the recent progress on the applications of electrospun nanofibers in enhanced localized cancer treatment. The potential challenges as well as the prospective for further development are also discussed.

1. Introduction

The research in therapeutic technologies for cancer, the deadliest disease to mankind, has been extensively endeavored. In the current times, radiotherapy and surgery remain as most common methodology for treating local and nonmetastatic tumors, whereas chemotherapy is the major strategy for metastatic cancers.[1]

Chemotherapy, which utilizes chemotherapeutic agents that are highly toxic to cancer cells, is a predominant therapeutic strategy for majority of cancer managements because of its superior efficiency.[2] Owing to a series of intrinsic drawbacks,[3] drug delivery systems (DDSs) were extensively explored to improve the stability, blood circulation and delivery efficacy of therapeutics. In general, DDSs enable the delivery of drugs in a more controlled way (release rate and time) and allow the preservation of drug concentration at a certain level within the valid therapeutic window. Systemic delivery drug systems (SDDSs) are based on particulate form, including nano/microparticles,[4] micelles,[5] and liposomes.[6] In general, tumor organ possesses enlarged interspace between endothelial cells of blood vessels induced by angiogenesis, and can retain particles at nanoscale dimensions during blood circulation. This phenomenon, known as enhanced permeation and retention (EPR), effectively facilitates the accumulation of nanoparticles at the tumor site before clearance by liver, spleen or kidney.[7] The particle size that can trigger this EPR effect ranges from 30 to 200 nm.[8]

However, SDDSs are often non-discriminating, and thus anticancer drugs circulate around the body.[9] In consequence, a maximum concentration of drug is initially reached during administration, followed by rapid clearance by biological system, leading to limited therapeutic efficacy and detrimental side effect.[10] Although researchers have made great effort in functionalizing nanostructured SDDSs with cancer-targeting molecules to avoid excessive uptaking by normal tissues,[11] the delivery efficiency to a solid tumor after administration remains as low as ~0.7 % (median) based on a recent 10-year literature survey.[12] There is a clear demand to explore new drug delivery vehicles with different functioning principles that enables improved delivery efficacy, reduced toxicity and superior drug release administration.

Localized drug delivery systems (LDDSs) originated in 1960s when therapeutic agent incorporated silicone rubber was implanted to ensure certain therapeutic efficiency.[13] The drug-loaded system implanted at the tumor site favors the localized drug delivery and avoids excessive drug circulation, enabling the suppression of side effect to normal tissues compared to particulate DDSs. The therapeutic dose at the cancerous zone can be maintained for a prolonged period while ensuring low systemic drug concentration. This not only improves anticancer efficacy but also avoids repeated drug administration.[14] There are several potential applications of LDDSs in cancer treatment. The first application is in treating the cancer patients with unsatisfactory conditions (i.e. elderly patients, patients with multiple diseases etc.). In this case, LDDSs loaded with anti-cancer drugs can be implanted into the tumor tissue through imaging system-aided positioning *via* minimally invasive surgery. The second application is to treat the tumors that are not readily surgically resected, such as pancreatic cancer, because of possible local infiltration and spreading. For patients

with such tumors, LDDSs which can deliver therapeutic agents to the tumor site locally can kill tumor cells and inhibit the cell proliferation with a great efficiency. The third application is to implant the drug-loaded LDDSs at the post-operative cavity site after tumor resection, aiming at eliminating residual cancer cells and preventing possible cancer recurrence. Therefore, this type of platform has gradually been recognized as a highly potential candidate to address the issues associated with current particulate administration of specific therapies.

A variety of forms of LDDSs have been explored, such as drug-eluting wafers, gels, rods and films.[14a] Nanofibers synthesized by electrospinning have presented unique characteristics, including (a) similar microstructure to extracellular matrix (ECM);[15] (b) high surface area;[16] (c) high porosity with interconnectivity which promotes cell adhesion, proliferation, drug delivery, and mass transport properties;[17] and (d) a wide selection of the matrix materials.[18] In addition, the development of advanced electrospinning techniques also provides new approaches for loading and releasing of insoluble drugs.

In 2006, Xu *et al.* reported a study of electrospun nanofibers for cancer therapy.[19] They mixed 1,3-bis(2-chloroethyl)-1-nitrosourea (BCNU) and poly(ethylene glycol)–poly($_L$-lactic acid) (PEG–PLLA) copolymer in chloroform and co-electrospun to form implantable BCNU embedded PEG–PLLA nanofibers. Nanofibers loaded with drug showed killing effect on rat glioma C6 cells in 72 h. In contrast, free BCNU lost cytotoxic activity after 48 h due to the instability. Later in the same year, Xie and Wang used electrospun mat to treat C6 gliomas.[20] By manipulating processing parameters, fibers with different diameters were fabricated successfully. Anticancer drug, Paclitaxel, was incorporated into electrospun PLGA nanofibers at a loading efficiency of more than 90 %. The study demonstrated that the release of drug could last for over 60 days, enabling high killing effect (~70%) of C6 Glioma cells in 72 h. Following the studies that ultilizing electrospun nanofibers in anti-cancer drug delivery,[21] a series of wide spreading investigations, regarding the exploration of new LDDSs for thermal therapy, gene therapy, photodynamic therapy, and combination therapy (Figure. 1), have been pursued thereafter.

2. Electrospinning

Electrospinning, derived from “electrostatic spinning”, is a method that materials in viscoelastic solution or melting state are formed into continuous fibers at a nano- or micro-scale dimensions. The setup of electrospinning is mainly made of a syringe pump, a spinneret, a high voltage power supply, and a collector (Figure. 2). The syringe loaded with material solution is equipped with an electro-conducting needle. The fluid at the tip tends to form a hemi-spherical droplet due to the confinement of surface tension. A high-voltage field, usually 1–30 kV, is supplied between the collector and the needle. When the voltage exceeds a threshold value when the electric repulsive force among the charges overcomes the surface tension of the droplet, the spherical shape is destabilized, and a conical charged jet of the solution is ejected from the apex of the cone, called ‘Taylor’ cone. The solution jet continues to accelerate and stretches into a form of long and thin fibers, accompanied with solvent evaporation. The electrospinning jet can be monitored by high speed camera. Various fibrous mats with controlled geometry can be generated by this technique.[22]

3. Electrospun nanofibers for chemotherapy

3.1. Single electrospun nanofibers for control drug delivery

3.1.1. Polymer nanofibers—Polymer nanofibers have recently raised great attention because of its enormous potential in separation industry, photonics, catalyst, electronics, enzyme immobilization, medical field and many others.[21a] Polymer, both natural and synthetic, is a key ingredient in the development of chemotherapeutic electrospun nanofibers due to their exceptional properties, such as light weight, mechanical flexibility, and chemical specificities.[23] Natural polymers present high biocompatibility, and some shows intrinsic antibacterial performances and ease of clinical functionalization.[24] Natural polymers for electrospinning include proteins (silk, gelatin, fibrin, albumin, collagen, etc.), polysaccharides (chitin, chitosan, cellulose, dextrose etc.), biopolymer derivatives and DNA. [25] Synthetic polymers, in turn, can be fabricated with manipulated compositions and properties to match specific applications.[26] Polymers such as poly(ethylene oxide) (PEO), poly(ε-caprolactone) (PCL), poly(lactic acid) (PLA), polydioxanone (PDS), and copolymers including poly(lactic-co-glycolic acid) (PLGA) and poly ($_L$-lactide-co-caprolactone) (PCLA) have been electrospun with tailored properties for drug delivery. In particular, biodegradable polymers, which can avoid a secondary operation to dislodge the implanted carrier, have attracted special attention in localized cancer therapy. A diversity of anticancer drugs including paclitaxel (PTX), epirubicin, dichloroacetate, 5-FU and camptothecin have been incorporated into electrospun polymer fibers and utilized for postoperative localized chemotherapy. The current polymer nanofibers LDDSs for chemotherapy are summarized in Table 1 below.

3.1.2. Ceramic nanofibers—Electrospinning was originally developed for synthesizing polymer-based nanofibers. Nowadays, advanced processing strategies, such as sol-gel chemistry, enable the incorporation of drug or biomolecules within ceramic nanofibers. Several studies have been undertaken to investigate the anticancer properties of drug loaded ceramic nanofibers. In addition, the extended functionalities were also uncovered due to the unique characteristics of inorganic nanofibers, which can hardly be achieved in polymeric materials.

For example, a series of Er doped strontium titanate ($SrTiO_3$, STO) nanofibers were synthesized for carrying DOX.[10] By the addition of surfactants with diverse types and concentrations into the precursor solution, STO nanofibers with controllable microstructural characteristics were synthesized. The nanofibers have the highest specific surface area, so they own tardy releasing kinetics and the highest DOX loading capacity. Consequently, the efficient *in vitro* killing effect to cancer cells of such nanofibers was induced. More importantly, the ratio of green to red emission (I_{550}/I_{660}) of upconversion STO nanofibers by 980 nm irradiation can be utilized to monitor the amount of DOX released based on the fluorescence resonance energy transfer (FRET) effect built between upconversion photoluminescent nanofibers and drug molecules. Rare earth doped $SrTiO_3$ nanofibers can also be utilized in stimuli-responsive drug delivery, enabling controlled drug release kinetics and optical monitoring functionalities.[59] This type of ceramic nanofibers with

ratiometrically monitoring functionality, have provided a promising platform for advanced localized tumor chemotherapeutic strategy.

3.2. Core-shell nanofibers for drug delivery

3.2.1. Characteristics—To form functional nanofibers with specific or multiple functions, various functional particles are incorporated into electrospun fibers. For example, to enhance therapeutic efficacy, drug-loaded carriers such as gold nanorods, silica nanoparticles, polymeric micelles and carbon nanotubes were incorporated into nanofibers for local cancer therapy. Compared with single drug loaded nanofibers, these core-shell structures have shown advantages such as prolonged action time and controlled drug release. Moreover, a series of new functionalities can be achieved by combining different materials in one fibrous scaffold.

3.2.2. Control of drug release kinetics—The ideal drug delivery system is expected to enable the temporally and spatially control of drug release.[60] The drug release of nanofibers occurs only at the target site due to its local implantation. For temporally controlled release, core-shell nanofibers provide a complex structure with multilayers for drug loading and releasing. Therefore, the release control can be achieved by tailoring the components in different layers that induces varied polymer degradation/erosion rates, drug dissolution rates, drug diffusion rates, drug physical desorption rates. In addition, by introducing stimuli-responsive constituent, the system can be responsive to the variation of environmental parameters including temperature, magnetic field, light, pH, which at last affect the drug release rate.

Yan *et al.* fabricated a core–shell nanofibrous mesh by coaxial electrospinning for chemotherapy, in which chitosan (CS) and polyvinyl alcohol (PVA) forms the shell and core layer, respectively.[61] When CS was crosslinked with glutaraldehyde (GA) vapor to suppress PVA swelling, the release of DOX drug in the core region was effectively governed. In addition to the uniform distribution of drug in core region, drugs can also be loaded into other multilayer structure. An implantable micelle-in-nanofiber platform with active-targeting property for localized cancer therapy was investigated by Yang *et al.*[62] They entrapped active-targeting DOX-loaded micelles (FM) into core-shell nanofibers (FM-Nanofiber), in which the core phase was the mixture solution of the micelles and poly (vinyl alcohol) (PVA) and the shell was gelatin solution (Figure. 3). It was found that DOX released from the FM inside dialysis bags reached 75 % in 48 h while cumulative release in the same time of FM-Nanofibers inside dialysis bags was only 40 %. The faster DOX release in the single micelle structure was because that the aqueous environment disturbed the thermodynamic stability of the polymeric micelles.[63] However, after the DOX-loaded micelles were encapsulated in nanofibers, the cross-linked gelatin shell, which acts as a barrier and prevents the disassembly of micelles encapsulated in the nanofiber matrix, can postpone the leaking of drug. The further *in-vivo* study confirmed that this active-targeting fibrous device could comparably suppress tumor growth due to the sufficient accumulation of anticancer drugs at the tumor site for prolonged time.

Similarly, Zhang *et al.* designed core-shell nanofibers for dual drug release.[64] $Pt_{(IV)}$ prodrug was reacted with PEG_{2k} units to form the amphiphilic $Pt_{(IV)}$ prodrug-backboned copolymer, $(PEG_{2k}–Pt_{(IV)})n$, *via* copper free click polymerization (Figure. 4). Then the copolymer was self-assembled into $Pt_{(IV)}$ micelles. With dichloroacetate (DCA), the micelles were electrospun together into PVA nanofibers. After implantation, PVA component can dissolve gradually at the tumor site, inducing fast release of $Pt_{(IV)}$ micelles and DCA. The diffusion of released DCA into cells resulted in cell apoptosis immediately. Meanwhile, $Pt_{(IV)}$ micelles were internalized by cancer cells *via* EPR effect, and reduced into toxic $Pt_{(II)}$ for killing tumor cells. The release of Pt exhibited a reduction and pH dual responsive behavior. As the tumor tissues have lower extracellular and intracellular pH as well as higher reducing substances level,[65] $Pt_{(IV)}$ would reacted into active $Pt_{(II)}$ and break the micelle structure around the tumor, thus reducing the accumulation of Pt in normal organs.

In addition to pH-responsive LDDSs, Li *et al.* fabricated a temperature-responsive nanogel-in-microfiber device *via* coaxial electrospinning.[66] Drug encapsulated poly-ethylene oxide (PEO) forms inner core, and the outer shell layer is made up of poly(ε-caprolactone) (PCL) and temperature responsive nanogels (Figure. 5). The nanogels consist of temperature sensitive PIPAAm that is copolymerized with acrylic acid (AAc). With the variation of environmental temperature, the nanogels in PCL matrix swell or shrink, leading to the disappearance or formation of channels between PCL and nanogel and thus the change of shell permeability. Therefore, the shell layer can act as a temperature-responsive valve for controlling the drug release. Methyl orange (MO) was firstly encapsulated into core part of the fibers as a drug model. The MO released rapidly at 40 °C, but slowed down at 20 °C through a cycle test, indicating the fully reversible thermo-triggered release. More drugs were released due to the switched-on state of the device, which consequently induced enhanced cancer cell death.

Li *et al.* reported the synthesis of hybrid electrospun nanofibers which can deliver anti-cancer drug controlled by near infrared (NIR) light.[67] The hybrid nanofibers were composed of poly (N-isopropylacrylamide) (PNIPAM), DOX loaded silica-coated gold nanorods ($Au@SiO_2$-DOX) and polyhedral oligomeric silsesquinoxanes (POSS). With NIR triggering, $Au@SiO_2$ particles heated up PNIPAM locally, inducing large-volume decrease by 83 % and accelerating the release of DOX. The released DOX could reduce the viability of Hela cells by ~97 % in a time period of 48 h. In this study, photothermal effect of gold nanorods were used to change the swelling behavior of PNIPAM, which in turn influenced the leakage of drug. The combination of hyperthermia and chemotherapy was demonstrated to induce enhanced therapeutic efficiency as well as decreased dose required. [21a]

pH value within microenvironment of cancerous tissues, infarctions, and other conditions associated with alkalosis and acidosis, varies.[68] Generally normal tissues and blood have a pH value of ~7.4, and tumor tissue has an extracellular pH of 5.8–7.2. The high presence of glycolysis in tumor cells under either anaerobic or aerobic conditions has been thought a main cause to the acidity, which facilitates invasiveness (metastasis) by deconstructing the ECM of surrounding normal tissues.[69] Samadi *et al.* incorporated graphene oxide/TiO_2/doxorubicin (GO/TiO_2/DOX) complex in electrospun chitosan/poly(lactic acid) (PLA)

nanofibers for delivering DOX and treating lung cancer.[70] The fibers with thicknesses of 30 and 50 μm presented initial burst release of DOX and subsequent sustained release. In addition, the release of DOX from nanofibers was faster in pH 5.3 than that in pH 7.4. The *in vitro* study indicated that the external magnetic field induced higher drug concentration at the target site, which consequently enhanced the proliferation inhibition of A549 lung cancer cells.

Hosseini *et al.* reported a PLA/carbon nanofiber (CNT)/Fe_3O_4 system for leukemia treatment.[71] They incorporated anticancer drug daunorubicin loaded carboxylated CNT/Fe_3O_4 composite into PLA nanofibers by electrospinning. Under a magnetic field, the drug concentration at the target site was increased. Meanwhile, pH-responsive drug release presented, where the faster release at pH of 5.5 was attributed to the protonation of carboxyl groups in nanofibers. The dual-responsive drug release improved the killing effect on K562 leukemia cells.

In addition to the studies of electrospun core-shell nanofibers for localized drug delivery with controlled release above, a series of publications, regarding LDDSs with varied fiber structure or surface chemistry but following similar principles, were documented in the literature in the past five years, as summarized in Table 2 below.

3.2.3. Multifunctional drug delivery—The unique structure characteristics of core-shell nanofibers facilitate multiple functions in cancer treatment. Luminescent materials are widely utilized in cancer therapy recently. Hou et al. incorporated upconversion luminescent $NaYF_4$:Yb^{3+}, Er^{3+} nanoparticles into electrospun SiO_2 nanofibers.[93] DOX was loaded onto the composite nanofibers and the release of DOX was pH-sensitive. The DOX loaded nanofibers showed similar inhibition on Hela cells as the free DOX. Furthermore, the rare earth doped nanofibers can emit strong luminescence under NIR light. The excellent bioimaging property on Hela cells of the composite nanofibers indicate the promise of core-shell electrospun nanofibers as a multifunctional platform for simultaneously treating and imaging cancer (Figure. 6).

Furthermore, Chen et al. investigated a multifunctional electrospun composite fibers for dual-drug delivery to kill hepatoma cells.[94] Core-shell upconversion nanoparticles of $NaGdF_4$:Yb/Er@$NaGdF_4$:Yb@mSiO_2-polyethylene glycol, loaded with DOX, were added into PCL/gelatin composite nanofibers loaded with indomethacin (MC) to form nanofibrous meshes via elelctrospinning. This nanoparticle-in-nanofiber structured dual-drug LDDS can effectively overcome drug burst release at certain degree and enhance tumor inhibition. Upconversion luminescence of composite fibers enabled the effective monitoring of in vivo DOX release. Furthermore, the feasibility of magnetic resonance imaging (MRI) effect was also confirmed due to the presence of paramagnetic Gd^{3+} ions (Figure. 7).

3.3. Surface modification for electrospun fibers

Surface modification of drug delivery systems has been a common strategy for enabling controlled drug delivery at the targeted site.[95] A number of research using individual or a combination of surface modifications has been carried out on electrospun fibers to control the release of immobilized anticancer drugs whilst preserving functionality. Jiang *et al.*

demonstrated that polydopamine coating may effectively manipulate the loading and releasing behavior of charged agents from electrospun PCL nanofibers under different pH values.[96] During polydopamine coating at pH 8.5, amino groups (-NH_2) cyclized and hydroxyl groups (-OH) remained after the reaction. Molecules containing hydroxyl groups can release hydrogen cations. Hence, the polydopamine modified PCL nanofibers liberated hydrogen cations and induced the negative charged surface in neutral environments. Correspondingly, hydroxyl groups were protonated, and the surface charge of fibers become neutral in acid. Therefore, the loading capacity of positive charged rhodamine 6G hydrochloride (R6G) and doxorubicin hydrochloride (DOX) was enhanced with increased pH values. The release kinetic was opposite to the loading behavior, in which the molecules were released more rapidly in an acidic environment than those at the high pH values. The *in vitro* MTT assay indicated that the DOX released at low pH value induced enhanced cancer cell death, indicating pH–responsive release. Following up, Yuan *et al.* reported a polydopamine modified elecctrospun fibrous membranes for controlled DOX loading and releasing.[97] The *in vivo* study demonstrated that both protein and mRNA levels of PDA-modified nanofibers have enhanced proapoptosis and necrosis-induced effect. Inspired by the work above, an approach to NIR and pH dual-triggered release of anticancer drug *via* electrospun fibers was developed recently.[98] Calcium titanate ($CaTiO_3$) nanomaterials with confirmed biocompatibility has demonstrated great potential for drug delivery in cancer treatment.[99] Yb, Er co-doped $CaTiO_3$ (CTO:Er,Yb) nanofibers, surface-modified with poly (acrylic acid) (PAA), were synthesized. Due to the electrostatic interaction between PAA molecules and DOX, the DOX loading capacity was remarkably increased. In addition, DOX released in a pH-dependent manner due to the protonation of the carboxyl groups of PAA molecules with the decreased pH value, and interestingly the release was monitored by upconversion photoluminescence spectra under 980 nm irradiation. Furthermore, the PAA coating also enabled NIR-triggered drug release due to the weak temperature rise and subsequent vibration of PAA chains when exposed under 808 nm irradiation (Figure. 8). Similar study was also reported in PAA modified CaF_2:Yb,Er@SiO_2 nanofibers.[100] The type of surface-functionalized nanofibers may have inspired researchers to focus on advanced protocols in cancer treatment.

4. Electrospun nanofibers for thermal therapy

The employment of heat has become one of the main strategies for cancer therapy since the 20^{th} century when a glowing tip of a firedrill was utilized for breast cancer treatment. [101] Hyperthermia, as a clinical method, is based on a selective tumor response under a moderate heating phenomenon, commonly in the region of 41–47 °C for 20–30 min.[102] Tumor cells are more susceptible to hyperthermia than their normal counterparts. Hyperthermia can cause reversible tumor cell damage by ‘softerning’ cell membranes and denaturing proteins, while the harm to healthy tissue is reversible.[103] Various heating sources, such as ultrasound,[104] radio frequency irradiation,[105] and microwaves,[106] have been used to induce heating of a specific target region. The utilization of electrospun fibrous scaffolds can overcome the challenge of hyperthermia to provide local heat at the tumor site while suppressing the injure of the surrounding normal tissues.

4.1. Photothermal therapy (PTT)

The precise spatiotemporal control of biologically relevant species delivery has been a hot spot in life science in recent years. Light, especially near-infared (NIR) light, within 'transparency window' for biological tissues, is an elegant on/off stimulus to achieve these criteria.[107] PTT using external light, preferably NIR light, induces heating to kill cancer cells and has recently attracted wide-spreading attention because of its relatively deep tissue penetration, simplicity, noninvasiveness, safety, oxygen independence and remote-controllable properties.[108] An ideal photothermal agent is expected to present strong NIR absorbance and capability in transferring the absorbed optical energy into thermal efficiently.[108a] In addition, the photothermal agent should be nontoxic in the dark to improve treatment efficacy without toxic side effects.[108a, 109] In the past decades, a large variety of PTT agents with certain light absorbance, good optical stability and outstanding photothermal efficiency have been developed.[110] The iconic advancement in this field includes gold nanostructures,[111] carbon nanomaterials,[112] metal sulfides and oxides,[113] and even organic materials.[114]

Cheng *et al* incorporated PEG modified gold nanorods (PEG-GNRs) into electrospun PLGA/ PLA-*b*-PEG membrane.[115] The polymer membrane in this platform served as the physical barrier on the surgical injury and a carrier for PEG-GNRs with excellent biocompatibility. When incubated with cancer cells, the PEG-GNRs liberated from the fibrous mat, and were subsequently internalized by cells (Figure. 9). Under 850 nm NIR irradiation, heat generation for the released PEG-GNRs was observed. The *in vitro* study showed that the PEG-GNR-incorporated mesh could selectively kill cancer cells and effectively suppress their proliferations.

In addition to LDDSs incorporated with Au nanoparticles, polyaniline nanoparticle is another promising photothermal agent, which can be embedded into PCL and gelatin (PG) nanofibers for tumor treatment.[116] Polyaniline nanoparticles absorb the optical energy of NIR light and generate heat when exposed to 808 nm irradiation, enabling ablation of cancer cell. The nanocomposite pieces were implanted directly into tumor in mice surgically to perform *in-situ* photothermal therapy. The *in vivo* examination demonstrated that polyaniline loaded PG composite had a remarkable inhibition on tumor growth by producing local heat to ablate tumor cells upon NIR irradiation. Furthermore, Mauro *et al.* investigated an implantable PCL electrospun nanofibers and tuned the surface physicochemical characteristics by nitrogen plasma activation. The nanofibers were functionalized with graphene oxide (GO), which was also a photothermal agent.[117] GO sheets were conjugated to the fibrous mesh through amide bond (Figure. 10). The GO deposition improved the selective adhesion and proliferation of cells, and enabled the photothermal ablation of the captured cancer cells *in situ* (~98 %), establishing the potential of GO-functionalized biomaterials for in situ killing metastatic cells.

In addition to direct therapeutic practice, the electrospun mats can also serve for a supplementary debridement treatment after surgical excision to clear the remaining asymptomatic tumor regions. To achieve the cutaneous defect healing after surgery and tumor therapy simultaneously, an electrospun micropatterned mats integrated with Cu_2S nanoflowers was fabricated recently (Figure. 11).[118] The fibrous membrane showed

controllable and excellent photothermal behavior under NIR irradiation. Skin tumor cells were effectively cleared, and the tumor growth was inhibited in mice. In addition, the density of fibers collected in the insulating area of the collector was lower, and thus the structure was loose, promoting the delivery of nutrient and oxygen to cells and the consequent ingrowth and migration of fibroblasts. More importantly, in addition to the tumor ablation effect of the Cu_2S nanoflowers in the membrane, the fibers facilitated the healing process of tumor-induced wounds due to the stimulation effect of Cu ions on the migration and proliferation of endothelial cells. The findings indicated that the Cu_2S-loaded mats combine enhanced skin tissue regeneration performance and cancer photothermal treatment effectively in one single platform.

However, it is noted that, due to the inevitable depth-dependent reduction of laser intensity, the heat distribution within tumor tissue is inhomogeneous, restricting the killing effect to the deep-located tumors.[119] In addition, the hyperthermia may induce possible inflammation and damage to healthy tissue.[120] The upregulation of the expression of heat shock protein (HSP) induced by PTT may increase the heat stress tolerance of cancer cells, limiting the photothermal therapeutic efficiency.[121]

4.2. Magnetic Hyperthermia (MHT)

Magnetic hyperthermia, which uses superparamagnetic iron oxide materials as a heating source, is an important technology of thermal cancer therapy.[122] Under an alternating magnetic field (AMF), magnetic materials are heated rapidly, resulted from the transfer of magnetic energy to thermal energy.[123] As tumor cells are more susceptible to heat than normal tissue, magnetic thermal therapy allows the local treatment of tumors without harmful effect to healthy tissues by placing iron oxide material-incorporated fibrous scaffold where cancer cells are located.[122] Owing to the superior tissue penetration ability of AMF, MHT can ablate tumors located in high depth. In addition, the contactless employment of AMF facilitates MHT to remotely treat tumors that are not accessible to PTT.[124] Lin *et al.* attempted to incorporate magnetic nanoparticles on/in chitosan nanofibers.[125] Upon application of AMF, the temperature of the solution containing magnetic chitosan nanofibers increased to 45 °C. The nanofibers hardly presented cytotoxicity but could generate a significant hyperthermia effect for killing cancer cells. In addition, iminodiacetic acid (IDA) was immobilized onto chitosan nanofibers to improve the formation of magnetic nanoparticles on nanofibers, and enhanced anticancer effect of IDA-conjugated nanofibers under AMF was demonstrated.[126]

Surface modification of magnetic nanofibers facilitates enhance cell attachment and consequent tumor suppressing performance. Huang *et al.* reported the synthesis of polystyrene (PS) magnetic electrospun fibers, loaded with 50 nm sized iron oxide nanoparticles (IONPs).[127] Under an AMF, the IONP-containing fibers generated efficient heating. Furthermore, collagen functionalization was carried out to improve the attachment of human ovarian cancer cells. All the attached cancer cells were killed when applied 10-minute alternating magnetic field, which was more efficient than the warm water bath. The well-controlled loading amount of IONPs and localization by magnetic resonance imaging *in vivo* endowed the magnetic electrospun fibers as a promising type of LDDSs for cancer

treatment. MHT has similar disadvantages as PTT, including the heat resistance, damage to healthy tissue and inhomogeneous heat distribution within tumor tissues.

5. Electrospun nanofibers for photodynamic therapy

Photodynamic therapy (PDT) relies on the use of reactive oxygen species (ROS) and free radicals, generated by a photosensitizer (PS), to induce phototoxicity. It is a rising oncologic therapeutic modality with specific spatiotemporal control and selectivity.[128] PDT generally requires three key components: photosensitizers, excitation light, and oxygen molecules.[129] Compared with typical cancer treatments including surgery, radiotherapy and chemotherapy, the main advantage of PDT is its inherent safety in the absence of light, no drug resistance, repeated treatment and minimal invasiveness.[130]

Conventional PDT induces relatively large amount of photosensitizer by intravenous, which may result in skin photosensitivity and high uptaking by normal cells. [23, 131] The use of nanofibrous scaffold for deliverying photosensitizers reduces the therapeutic dosage significantly. Studies of photosensitizer loaded nanofibers in the application of antibacterial, [132] catalysis,[133] water treatment[134] and wound healing[135] have been reported extensively. Electrospun nanofibers for cancer PDT can achieve considerable selective therapeutic effect by simply focusing the light on the scaffold-localized tumor region. [128a, 136] Severyukhina *et al.* reported a type of photosensitizer-loaded electrospun fibers for photodynamic cancer therapy.[131] Chitosan/PEO nanofibers consisting of different Photosens were synthesized by electrospinning. The physically adsorbed Photosens initially released with the swelling of the nanofibers. A relatively tardy release was detected due to the degradation of nanofiber complex. Under 675 nm laser irradiation, the metabolic activity of scaffold-treated human mammary gland T-47D cancer cells was significantly suppressed without recovery. In addition, limited illuminated area could control the phototoxic effect spatially, indicting the enhanced topical photodynamic cancer therapy. Similarly, purpurin-18 was incorporated into electrospun PLLA nanofibers with sound biocompatibility by Wu *et al.*[23] Satisfactory interaction and integration of both human esophageal cancer ECA109 cells and human hepatocellular carcinoma SMMC 7721 cells with the surrounding fibers were observed. MTT assays exhibited that the killing effect on cancer cells occurred immediately after PDT when exposed to a 702 nm laser light.

However, LDDSs for PDT also suffer several challenges. Firstly, most organic photosensitizers rely on oxygen for $^1O_2$ generation, which only performs well in oxygen-rich environment and thus fails to treat hypoxic tumors.[137] In addition, the excitation wavelength of most photosensitizers are in the ultraviolet and visible region,[138] which presents low tissue penetration, thus failing to treat deep tumors. Furthermore, the lifetime of singlet oxygen in water is approximately a few microseconds. Its half-life in biological systems is less than 40 ns, and the diffusion distance is short. [139] Its active radius is ~20 nm,[140] so it can only react with substances near the photosensitizers.

6. Electrospun nanofibers for cancer gene therapy

With the growing knowledge of tumor immunology, cancer gene therapy, which aims to treating cancers *via* therapeutic nucleic acids, have gained considerable clinical success recently.[141] Compared to chemotherapy, gene therapy aims to repair the cause of cancer diseases by modulating the dysregulated genes and their expressions rather than remitting disease symptoms.[142] Gene therapy includes the delivery of plasmid DNA (pDNA) to replace mutated or supplement down-regulated genes, and/or nucleic fragments such as micro RNA (miRNA), short hairpin RNA (shRNA), or small interfering RNA (siRNA) to interfere the protein expression of any target gene.[143] The degradation of naked nucleic acids occurs due to the presence of various biomolecules in the blood stream, such as nucleases.[142] Whereas, the ECM-like structure of nanofibers reduces the distance between cancer cells and therapeutic genes being delivered. It can maintain a relatively high content of therapeutic genes at the tumor site while ensuring certain gene activity and low systemic toxicity. Following this principle, Achille *et al.* adopted biodegradable electrospun PCL nanofibers for delivering gene to treat breast cancer.[144] A plasmid encoding short hairpin RNA (shRNA), which can suppress the level of the cell cycle specific protein, cyclin-dependent kinase 2 (Cdk2), was combined into fibrous scaffold. The gradually released of functioned shRNA from PCL nanofibers effectively silenced Cdk2, leading to the destruction of the cancer cell cycle and the inhibition of the breast cancer cells proliferation. The study indicates that gene therapy in combination with electrospun nanofibers, which can provide ECM-mimicking environments and controllable gene delivery, can be a highly potential substitute to specifically target a diversity of cancer cells. However, electrospun nanofibers may have poor capability in intracellular delivery of therapeutic genes, inducing low gene silencing effect. In addition, the safety concern regarding the adverse reactions on the body's immune system ought to be systematically evaluated and addressed. Following the introduction of current LDDSs for solo cancer therapy, a direct cross comparison of the advantages and challenges of each type is provided (Table 3).

7. Electrospun nanofibers for combination therapy

Combination cancer therapy has raised great attention in clinical practice to overcome the disadvantages associated with single cancer treatments and achieved significant success. For example, prolonged drug release using LDDSs for solo chemotherapy may induce the strong resistance of cancer cells against chemotherapeutics, known as multiple drug resistance (MDR)[145]. In addition, chemotherapy may induce inevitable side effects at a certain degree. In contrast, combination cancer therapy, the co-delivery of two or more anticancer agents simultaneously or a combination of therapeutic approaches, can build a synergsitic platfom for treating MDR cancer cells with lower drug concentrations, achieving an enhanced combined therapeutic efficiency. Therefore, recent studies have also been focused on the multifunctional nanofibers combining two or even more theraputic techniques aiming at enhanced cancer treatment.

7.1. Chemotherapy & photothermal

The combination of photothermal therapy and chemotherapy can increase the inactivation of tumor cells owing to the following reasons: (a) High temperature changes the blood perfusion of capillaries and accelerates drug release, thus changing the distribution of drugs in the tissue and increasing the concentration of drugs in the sites where the drugs can not reach.[146] (b) High temperature destroys the stability of tumor cells, increases the permeability of cell membrane, and thus facilitates cellular uptaking of drugs. Meanwhile, the hyperthermia induces the dysfunction of cell membrane, hypoxia, and anaerobic glycolysis. In consequence, the pH value decreases, and the activity of drug is enhanced in an acidic environment. (c) High temperature increases the cytotoxic effect of chemotherapeutic drugs. (d) The hyperthermia enhances the sensitivity of MDR cells to anti-cancer drugs.[147]

Zhang et al. attempted to incorporate doxorubicin (DOX) and multiwalled carbon nanotubes (MWCNTs) into electrospun PLLA nanofibers to combine chemotherapy and photothermal therapy.[148] MWCNT is an effective photothermal agent which absorbs NIR light with a wide wavelength range. It was found that the 808 nm NIR illumination did not only trigger DOX release, but also induce the localized overheating of fibers-covering tumor site, resulting in enhanced inhibition of tumor growth. Similarly, the integration of chemotherapy and photothermal was also observed in another platform, in which DOX loaded Cu_9S_5@mSiO_2 nanoparticles were embedded into electrospun PCL and gelatin nanofibers (Figure. 12). [149] The multifunctional composite fibers were surgically implanted into the tumor site to realize the orthotopic combination therapy. The in vivo study showed that the combined chemotherapy/photothermal therapy presented a significantly enhanced tumor inhibition effect comparing to either chemotherapy or photothermal treatment.

7.2. Chemotherapy & magnetic-thermal

Similar to PTT, magnetic thermal therapy induces local hyperthermia to enhance drug release and increases intracellular drug concentration for improved chemotherapy efficacy, resulting in synergistic MHT/chemotherapy.[150] Furthermore, the precise control of drug release by controlling the parameters of AMF is highly promising to achieve on-demand combined MHT/chemotherapy. This may enhance the treatment efficacy with minimal side effects. Nejad et al. investigated mussel-activated electrospun nanofibers loaded with IONPs and bortezomib (BTZ) for hyperthermic chemotherapy.[151] The nanofiber matrix was based on mussel- activated copolymer, poly(methyl methacrylate-codopamine methacrylamide) p(MMA-co-DMA) (MADO) (Figure. 13). The catechol moieties of surface-functionalized fibers can bind and release BTZ in a pH-dependent manner. The IONP-incorporated magnetic nanofibers displayed a remarkable heating property, and a long-lasting cyclic heating ability under an AMF. These implantable magnetic nanofibers enabled both repetitive hyperthermia therapy and tumor-specific drug release synergistically. In vitro studies showed that the BTZ-loaded magnetic nanofibers presented an excellent synergistic therapeutic efficacy for cancer treatment. A follow-on study by this group demonstrated a magnetic nanofiber (MNF) system based on PLGA nanofibers functionalized using dopamine and conjugated with BTZ (Figure. 14), and this type of LDDS can effectively

enable highly controlled BTZ release and hyperthermal phenomenon for cancer treatment. [152]

Kim *et al.* dispersed MNPs and DOX in temperature-responsive polymers (Figure. 15).[153] A mixture of magnetite (Fe_3O_4) and maghemite (γ-Fe_2O_3) MNPs were selected because of the instability of solo magnetite in oxidation. The thermal curable nanofiber was synthesized by electrospinning copolymer of NIPAAm and N-hydroxymethylacrylamide (poly(NIPAAm-coHMAAm)). Under high temperature, the crosslink of methylol group in HMAAm occurred by self-condensation. When AMF was provided (signal is 'ON'), the MNPs generated heat and resulted in the deswelling and collapse of polymer networks. Altering 'ON-OFF' switches of AMF, the swelling ratio of nanofiber changed. Correspondingly, the release of DOX showed in an 'ON-OFF' manner in response to AMF. Due to the combined effect of hyperthermal and drug, 70 % of cell death was observed in only 5 min when human melanoma cells were incubated with this delivery system. These smart nanofibers with dynamically and reversibly changeable structures can functionalize as a switchable hyperthermia implant as well as a manipulative drug carrier simultaneously by simply altering the AMF signal.

7.3. Chemotherapy & gene therapy

Cancer cells tend to develop MDR after frequent administration of high doses, which induces the ineffectiveness of chemotherapy. By certain type of siRNA, gene therapy can suppress the expression of MDR-related or anti-apoptotic proteins (Plk-1,[154] MRP1,[155] Bcl-2[156]) for enhancing the sensitivity of cancer cells toward chemotherapeutics, which paves the way for gene-based synergistic cancer therapy. The strategy combining the chemotherapy and gene therapy has been considered as a highly potential protocol for enhanced cancer treatment recently.[157] The blooming development of investigation in this particular technology is being extensively carried out. Sukumar *et al.* investigated a bioactive core-shell bPEI-PEO nanofiber scaffold by electrospinning for transporting cytosine deaminase-uracil phosphoribosyl transferase (CD::UPRT) (shell) suicide gene and simultaneously controlled delivery of anticancer prodrug 5-Fluorocytosine (5-FC) (core) (Figure. 16).[158] The Rhodamine B (RhoB)-bPEI-pDNA (plasmid DNA) (short as 'RBP') complex was mixed with PEO and bPEI solution as a shell and were initially released during incubation. Transfection and the expression of the suicide gene then occurred, followed by the release of prodrug. The results indicated that the scaffold activated the apoptosis of lung cancer cells (A549) by suicide gene therapy at phenotypic and genotypic levels. The simultaneous delivery of suicide gene and prodrug drastically enhanced anticancer efficacy.

Che *et al.* reported an approach combining drug and gene delivery for treating liver cancer. [159] In this work, nanoparticles containing disulfide cross-linked PEI (ssPEI) and anticancer gene microRNA-145 were grafted onto paclitaxel (PTX) loaded electrospun poly(ε-caprolactone) (PCL) nanofibers. The composite nanofibers exhibited time-dependent PTX and miR-145 release. The suppression of cancer cell growth by drug and gene co-delivery nanofibers was remarkably enhanced, indicating the synergistic effect. Furthermore, Lei *et al.* electrospun PLGA fibers for delivery drug and gene to treat malignant brain tumor.[160] An RNAi plasmid, aiming to suppress the expression of an important proteinase regulating

brain tumor invasion and angiogenesis, matrix metalloproteinase-2 (MMP-2), was complexed with polyethylenimine (PEI). Anticancer drug paclitaxel as well as the RNAi plasmid was encapsulated in PLGA fibers, and a sustained release of gene and drug was demonstrated. The RNAi plasmid released was active in transfecting cancer cells, and the MMP-2 was downregulated, resulting in the inhibition of tumor angiogenesis and invasion. The drug/gene dual delivery induced more effective tumor regression compared to the solo chemotherapy.

7.4. Photothermal & photodynamic

An efficient photodynamic process requires three major components, including photosensitizers, oxygen and light.[161] However, hypoxic tumor microenvironment leads to low productivity of ROS and hence restricts PDT therapeutic efficacy.[137a] As mild hyperthermia not only increases the membrane permeability to improve the cellular uptake of photosensitizers but also accelerates the blood flow to increase the vascular O_2 concentration, enhancing the ROS production.[162] Therefore, the hyperthermia-enhanced intracellular ROS generation leads to synergistic PDT/PTT via the integration of photothermal agents and photosensitizers within one LDDS. However, in the combination of PTT and PDT, it is inconvenient to activate the photothermal agents and photosensitizers using different wavelengths of lights, which also increases the equipment/time cost and undermines their synergistic interactions.[137b] A synergistic anticancer platform based on electrospun Yb,Er-codoped $CaTiO_3$ (CTO) nanofibers, which was co-conjugated with gold nanorods (AuNRs) and Rose Bengal (RB), was recently investigated for combined photothermal/photodynamic treatment (Figure. 17).[163] The absorption spectra of AuNRs and RB matched well with the red and green emissions of upconversion photoluminescent CTO nanofibers, respectively. Therefore, a single NIR (980 nm) laser can initiate PTT and PDT simultaneously. The *in vitro* study confirmed that the combined PTT/PDT therapeutic platform exhibited remarkably enhanced inhibition of Hep G2 cancer cell growth. This study may also provide another way of thinking in designing advanced LDDSs for combination cancer treatment.

8. Summary and outlook

In the past ten years, the research in electrospun nanofibers as a localized cancer treatment platform has witnessed a blooming development. This type of implantable LDDSs has been generally recognized as a highly potential therapeutic system for tumor treatments. However, a series of challenges remain to be tackled before they can be considered for clinical trials. The essential one is that the secondary removal surgery is required as most of current LDDSs are not biodegradable. The following challenge is then the potential hazard of residual solvents. For polymeric nanofibers, the common solvents used in electrospinning precursor process, such as dimethylformamide (DMF), acrylic acid, chloroform, dichloromethane (DCM), tetrahydrofuran (THF), hexafluoroisopropanol (HFIP), and 2,2,2-trifluoroethanol (TFE), present certain toxicity. Thirdly, when ceramic nanofibers with poor mechanical strength and flexibility are employed as LDDSs, they can hardly serve as free-standing structures over a large area. Additional concerns, such as industrial scale-up of

LDDSs, incompatibility between drugs and matrix materials and optimized drug release, ought to be addressed before this technology is brought into clinical practice.

From the perspective of fundamental research, to combat future clinical demands, two scientific breakthroughs are expected in addition to the development of new therapeutic strategies responding to tumor microenvironment. One is biodegradable nanofibers, which can degrade gradually in the body after its service in cancer treatment, thus avoiding repeated surgery for removal. Such biodegradable system has attracted special attention in localized cancer therapy. Secondly but more importantly, the intrinsic drawback of implantable electrospun nanofibers is the diffusion mechanism of the therapeutic molecules released from fibers into cancer cells at the diseased site, that may markedly hinder the cellular uptake efficacy and therefore the therapeutic efficiency. Particularly, for gene therapy where the genes are expected to be effectively internalized by tumor cells, the therapeutic gene released from electrospun fibers diffuses into tumor microenvironment, but the uptake efficiency of gene remains low due to the absence of gene carrier for intracellular transportation. The combination of nanofibers and nanoparticles (as gene carried for cell internalization) is being raised to be a highly potential localized gene therapy. In this system, the implanted fibrous mesh can deliver abundant therapeutic molecules loaded nanoparticles into cancerous region in a controlled manner, and subsequently the nanoparticles released can effectively transport the loaded molecules into tumor cells and trigger the expected treatment.

Overall, this review has provided a comprehensive glance of recent cutting-edge research in electrospun fibers for tumor therapy. One, that can be anticipated, is this particular type of advanced platform is launching a blooming era of developing new technologies for enhanced cancer treatment.

Acknowledgements

This work was financially supported by the National Nature Science Foundation of China (51672247 and 51673168), the 111 programs of China (B16042), the Major State Research Program of China (2016YFC1101900 and 2016YFA0100900), and Zhejiang Provincial Natural Science Foundation of China (LZ16E030001). CBM also would like to acknowledge the financial support from National Institutes of Health (CA195607).

Biography

Dr. Xiang Li holds a Ph.D. degree in Biomedical Materials from University College London (UCL), UK. At present, he serves as an Associate Professor at School of Materials Science and Engineering, Zhejiang University. His research interest focuses on the design and synthesis of nanoscale biomaterials for tissue engineering, cancer therapy and diagnosis. He has so far published over 90 peer-review journal papers.

Dr. Chuanbin Mao received his PhD in 1997 from Northeastern University in China. He has published over 180 peer-reviewed publications and about 10 book chapters. He is a fellow of the Royal Society of Chemistry (FRSC). He has won multiple awards including US National Science Foundation CAREER award. His research is now focused on phage display, nanobiotechnology, biomaterials, cancer nanomedicine, and regenerative medicine.

Prof. Gaorong Han received his Ph.D. degree from Zhejiang University in 1989. He is a Professor in School of Materials Science and Engineering at Zhejiang University. His research interest covers functional nanostructures for cancer therapy, tissue engineering, energy saving and conversion applications. He has published over 200 peer-reviewed publications. He also serves as the deputy chair of Materials Research Society of China.

References

[1]. Fonseca AC; Serra AC; Coelho JFJ, Epma Journal 2015, 6, 22. [PubMed: 26605001]

[2]. Qin S-Y; Zhang A-Q; Cheng S-X; Rong L; Zhang X-Z, Biomaterials 2017, 112, 234. [PubMed: 27768976]

[3]. a) Cho K; Wang X; Nie S; Chen Z; Shin DM, Clin. Cancer. Res 2008, 14, 1310; [PubMed: 18316549] b) Singh M; Kundu S; Sreekanth V; Motiani RK; Sengupta S; Srivastava A; Bajaj A, Nanoscale 2014, 6, 12849. [PubMed: 25227567]

[4]. a) Li Z; Hu Y; Howard KA; Jiang T; Fan X; Miao Z; Sun Y; Besenbacher F; Yu M, ACS Nano 2016, 10, 984; [PubMed: 26655250] b) Li Y; Zhou Y; Gu T; Wang G; Ren Z; Weng W; Li X; Han G; Mao C, Particle & Particle Systems Characterization 2016, 33, 896; [PubMed: 28670098] c) Li Y; Zhou Y; Li X; Sun J; Ren Z; Wen W; Yang X; Han G, RSC Advances 2016, 6, 38365. [PubMed: 27774143]

[5]. Li W; Peng J; Tan L; Wu J; Shi K; Qu Y; Wei X; Qian Z, Biomaterials 2016, 106, 119. [PubMed: 27561883]

[6]. a) Feng L; Gao M; Tao D; Chen Q; Wang H; Dong Z; Chen M; Liu Z, Adv. Funct. Mater 2016, 26, 2207;b) Ngweniform P; Abbineni G; Cao B; Mao C, Small 2009, 5, 1963. [PubMed: 19415651]

[7]. Albanese A; Tang PS; Chan WCW, Annu. Rev. Biomed. Eng 2012, 14, 1. [PubMed: 22524388]

[8]. Jain RK; Stylianopoulos T, Nature reviews Clinical oncology 2010, 7, 653.

[9]. Soussan E; Cassel S; Blanzat M; Rico-Lattes I, Angew. Chem. Int. Ed 2009, 48, 274.

[10]. Fu Y; Chen X; Mou X; Ren Z; Li X; Han G, ACS Biomater.-Sci. Eng 2016, 2, 652.

[11]. Huang S; Duan S; Wang J; Bao S; Qiu X; Li C; Liu Y; Yan L; Zhang Z; Hu Y, Adv. Funct. Mater 2016, 26, 2532.

[12]. Wilhelm S; Tavares AJ; Dai Q; Ohta S; Audet J; Dvorak HF; Chan WC, Nature Reviews Materials 2016, 1, 16014.

[13]. Folkman J; Long DM, J. Surg. Res 1964, 4, 139. [PubMed: 14130164]

[14]. a) Wolinsky JB; Colson YL; Grinstaff MW, J. Controlled Release 2012, 159, 14;b) De Souza R; Zahedi P; Allen CJ; Piquette-Miller M, Drug Delivery 2010, 17, 365; [PubMed: 20429844] c) Ho EA; Soo PL; Allen C; Piquette-Miller M, J. Controlled Release 2007, 117, 20.

[15]. Nair LS; Bhattacharyya S; Laurencin CT, Expert Opinion on Biological Therapy 2004, 4, 659. [PubMed: 15155157]

[16]. Xue J; Xie J; Liu W; Xia Y, Acc. Chem. Res 2017, 50, 1976. [PubMed: 28777535]

[17]. Jiang S; Lv L-P; Landfester K; Crespy D, Acc. Chem. Res 2016, 49, 816. [PubMed: 27135135]

[18]. Goyal R; Macri LK; Kaplan HM; Kohn J, J. Controlled Release 2016, 240, 77.

[19]. Xu X; Chen X; Xu X; Lu T; Wang X; Yang L; Jing X, J. Controlled Release 2006, 114, 307.

[20]. Xie J; Wang C-H, Pharm. Res 2006, 23, 1817. [PubMed: 16841195]

[21]. a) Thakkar S; Misra M, Eur. J. Pharm. Sci 2017, 107, 148; [PubMed: 28690099] b) Balaji A; Vellayappan MV; John AA; Subramanian AP; Jaganathan SK; Supriyanto E; Razak SIA, RSC Advances 2015, 5, 57984;c) Aberoumandi SM; Mohammadhosseini M; Abasi E; Saghati S; Nikzamir N; Akbarzadeh A; Panahi Y; Davaran S, Artificial Cells, Nanomedicine, and Biotechnology 2017, 45, 1058.

[22]. Wang X; Ding B; Yu J; Wang M, Nano Today 2011, 6, 510.

[23]. Wu H.-m.; Chen N; Wu Z-M; Chen Z-L; Yan Y-J, J. Biomater. Appl 2013, 27, 773. [PubMed: 22090428]

[24]. Hu X; Liu S; Zhou G; Huang Y; Xie Z; Jing X, J. Controlled Release 2014, 185, 12.

[25]. Bhardwaj N; Kundu SC, Biotechnol. Adv 2010, 28, 325. [PubMed: 20100560]

[26]. a) Ulery BD; Nair LS; Laurencin CT, J. Polym. Sci., Part B: Polym. Phys 2011, 49, 832;b) Nair LS; Laurencin CT, Polymers as Biomaterials for Tissue Engineering and Controlled Drug Delivery. In Tissue Engineering I, Lee K; Kaplan D, Eds. Springer Berlin Heidelberg: Berlin, Heidelberg, 2006; pp 47;c) Nair LS; Laurencin CT, Prog. Polym. Sci 2007, 32, 762.

[27]. Yohe ST; Herrera VLM; Colson YL; Grinstaff MW, J. Controlled Release 2012, 162, 92.

[28]. Li G; Chen Y; Cai Z; Li J; Wu X; He X; Zhao Z; Lan P; Li Y, Journal of Materials Science 2013, 48, 6186.

[29]. Chen P; Wu Q-S; Ding Y-P; Chu M; Huang Z-M; Hu W, European Journal of Pharmaceutics and Biopharmaceutics 2010, 76, 413. [PubMed: 20854905]

[30]. Zhu X; Ni S; Xia T; Yao Q; Li H; Wang B; Wang J; Li X; Su W, J. Pharm. Sci 2015, 104, 4345. [PubMed: 26505475]

[31]. Vashisth P; Sharma M; Nikhil K; Singh H; Panwar R; Pruthi PA; Pruthi V, 3 Biotech 2015, 5, 303.

[32]. Ignatova M; Yossifova L; Gardeva E; Manolova N; Toshkova R; Rashkov I; Alexandrov M, Bioact J. Compatible Polym 2011, 26, 539.

[33]. Zhang J; Wang X; Liu T; Liu S; Jing X, Drug Delivery 2016, 23, 784.

[34]. Sedghi R; Shaabani A; Mohammadi Z; Samadi FY; Isaei E, Carbohydr. Polym 2017, 159, 1. [PubMed: 28038737]

[35]. Ranganath SH; Wang C-H, Biomaterials 2008, 29, 2996. [PubMed: 18423584]

[36]. Xie J; Tan RS; Wang C-H, Journal of Biomedical Materials Research Part A 2008, 85A, 897.

[37]. Amna T; Barakat NA; Hassan MS; Khil M-S; Kim HY, Colloids Surf. Physicochem. Eng. Aspects 2013, 431, 1.

[38]. Laiva AL; Venugopal JR; Karuppuswamy P; Navaneethan B; Gora A; Ramakrishna S, Int. J. Pharm 2015, 483, 115. [PubMed: 25681729]

[39]. Sridhar R; Ravanan S; Venugopal JR; Sundarrajan S; Pliszka D; Sivasubramanian S; Gunasekaran P; Prabhakaran M; Madhaiyan K; Sahayaraj A; Lim KHC; Ramakrishna S, Journal of Biomaterials Science, Polymer Edition 2014, 25, 985. [PubMed: 24865590]

[40]. Sampath M; Lakra R; Korrapati P; Sengottuvelan B, Colloids Surf., B 2014, 117, 128.

[41]. Lu T; Jing X; Song X; Wang X, J. Appl. Polym. Sci 2012, 123, 209.

[42]. Toshkova R; Manolova N; Gardeva E; Ignatova M; Yossifova L; Rashkov I; Alexandrov M, Int. J. Pharm 2010, 400, 221. [PubMed: 20816737]

[43]. Jain S; Meka SRK; Chatterjee K, ACS Biomater.-Sci. Eng 2016, 2, 1376.

[44]. Wang C; Ma C; Wu Z; Liang H; Yan P; Song J; Ma N; Zhao Q, Nanoscale research letters 2015, 10, 439. [PubMed: 26573930]

[45]. Shanmuga Sundar S; Sangeetha D, J. Mater. Sci. Mater. Med 2012, 23, 1421. [PubMed: 22476650]

[46]. Liu S; Zhou G; Liu D; Xie Z; Huang Y; Wang X; Wu W; Jing X, J. Mater. Chem. B 2013, 1, 101.

[47]. Liu D; Wang F; Yue J; Jing X; Huang Y, Drug Delivery 2015, 22, 136. [PubMed: 24359441]

[48]. Liu D; Liu S; Jing X; Li X; Li W; Huang Y, Biomaterials 2012, 33, 4362. [PubMed: 22425553]

[49]. Ma G; Liu Y; Peng C; Fang D; He B; Nie J, Carbohydr. Polym 2011, 86, 505.

[50]. Guimarães PP; Oliveira MF; Gomes AD; Gontijo SM; Cortés ME; Campos PP; Viana CT; Andrade SP; Sinisterra RD, Colloids Surf., B 2015, 136, 248.

[51]. Kim Y-J; Park MR; Kim MS; Kwon OH, Mater. Chem. Phys 2012, 133, 674.

[52]. Ding Q; Li Z; Yang Y; Guo G; Luo F; Chen Z; Yang Y; Qian Z; Shi S, Drug Delivery 2016, 23, 2677. [PubMed: 26171813]

[53]. Chen P; Wu Q.-s.; Ding Y; Zhu Z.-c., Nano 2011, 06, 325.

[54]. Xie C; Li X; Luo X; Yang Y; Cui W; Zou J; Zhou S, Int. J. Pharm 2010, 391, 55. [PubMed: 20170717]

[55]. Salehi R; Irani M; Rashidi M-R; Aroujalian A; Raisi A; Eskandani M; Haririan I; Davaran S, Designed Monomers and Polymers 2013, 16, 515.

[56]. Zong S; Wang X; Yang Y; Wu W; Li H; Ma Y; Lin W; Sun T; Huang Y; Xie Z; Yue Y; Liu S; Jing X, European Journal of Pharmaceutics and Biopharmaceutics 2015, 93, 127. [PubMed: 25843238]

[57]. Xu X; Chen X; Wang Z; Jing X, European Journal of Pharmaceutics and Biopharmaceutics 2009, 72, 18. [PubMed: 19027067]

[58]. Liu S; Wang X; Zhang Z; Zhang Y; Zhou G; Huang Y; Xie Z; Jing X, Nanomed. Nanotechnol. Biol. Med 2015, 11, 1047.

[59]. a) Fu Y; Fang C; Ren Z; Xu G; Li X; Han G, Chem-Eur J 2017, 23, 2423; [PubMed: 27943465] b) Fu Y; Li X; Sun C; Ren Z; Weng W; Mao C; Han G, ACS Appl. Mater. Interfaces 2015, 7, 25514. [PubMed: 26544158]

[60]. Weng L; Xie J, Curr. Pharm. Des 2015, 21, 1944. [PubMed: 25732665]

[61]. Yan E; Fan Y; Sun Z; Gao J; Hao X; Pei S; Wang C; Sun L; Zhang D, Materials Science and Engineering: C 2014, 41, 217. [PubMed: 24907754]

[62]. Yang G; Wang J; Wang Y; Li L; Guo X; Zhou SB, ACS Nano 2015, 9, 1161. [PubMed: 25602381]

[63]. Owen SC; Chan DPY; Shoichet MS, Nano Today 2012, 7, 53.

[64]. Zhang Z; Wu Y; Kuang G; Liu S; Zhou D; Chen X; Jing X; Huang Y, J. Mater. Chem. B 2017, 5, 2115.

[65]. a) Webb BA; Chimenti M; Jacobson MP; Barber DL, Nat. Rev. Cancer 2011, 11, 671; [PubMed: 21833026] b) Brown JM; Wilson WR, Nature reviews. Cancer 2004, 4, 437. [PubMed: 15170446]

[66]. Li L; Yang G; Zhou G; Wang Y; Zheng X; Zhou S, Advanced Healthcare Materials 2015, 4, 1658. [PubMed: 25998801]

[67]. Li Y-F; Slemming-Adamsen P; Wang J; Song J; Wang X; Yu Y; Dong M; Chen C; Besenbacher F; Chen M, Journal of Tissue Engineering and Regenerative Medicine 2017, 11, 2411. [PubMed: 27241487]

[68]. Chen M; Li Y-F; Besenbacher F, Advanced Healthcare Materials 2014, 3, 1721. [PubMed: 24891134]

[69]. Oh KT; Yin H; Lee ES; Bae YH, J. Mater. Chem 2007, 17, 3987.

[70]. Samadi S; Moradkhani M; beheshti H; Irani M; Aliabadi M, Int. J. Biol. Macromol 2017.

[71]. Hosseini L; Mahboobnia K; Irani M, International Journal of Polymeric Materials and Polymeric Biomaterials 2016, 65, 176.

[72]. Shao S; Li L; Yang G; Li J; Luo C; Gong T; Zhou S, Int. J. Pharm 2011, 421, 310. [PubMed: 21983092]

[73]. Anaraki NA; Rad LR; Irani M; Haririan I, J. Appl. Polym. Sci 2015, 132, 41286.

[74]. Ardeshirzadeh B; Anaraki NA; Irani M; Rad LR; Shamshiri S, Materials Science and Engineering: C 2015, 48, 384. [PubMed: 25579938]

[75]. Chen M; Feng W; Lin S; He C; Gao Y; Wang H, RSC Adv 2014, 4, 53344.

[76]. Dai J; Jin J; Yang S; Li G, Materials Research Express 2017, 4, 075403.

[77]. Han D; Sasaki M; Yoshino H; Kofuji S; Sasaki AT; Steckl AJ, Drug Deliv J. Sci. Technol 2017, 40, 45.

[78]. Huang H-H; He C-L; Wang H-S; Mo X-M, Journal of Biomedical Materials Research Part A 2009, 90A, 1243.

[79]. Irani M; Mir Mohamad Sadeghi G; Haririan I, Int. J. Biol. Macromol 2017, 97, 744. [PubMed: 28109815]

[80]. Irani M; Sadeghi GMM; Haririan I, Materials Science and Engineering: C 2017, 75, 165. [PubMed: 28415451]

[81]. Liu W; Wei J; Chen Y, New J Chem 2014, 38, 6223.

[82]. Luo X; Xie C; Wang H; Liu C; Yan S; Li X, Int. J. Pharm 2012, 425, 19. [PubMed: 22265915]

[83]. Lv G; He F; Wang X; Gao F; Zhang G; Wang T; Jiang H; Wu C; Guo D; Li X; Chen B; Gu Z, Langmuir 2008, 24, 2151. [PubMed: 18193905]

[84]. Qiu K; He C; Feng W; Wang W; Zhou X; Yin Z; Chen L; Wang H; Mo X, J. Mater. Chem. B 2013, 1, 4601.

[85]. Saravanabhavan SS; Dharmalingam S, Chem. Eng. J 2013, 234, 380.

[86]. Wei J; Hu J; Li M; Chen Y; Chen Y, RSC Advances 2014, 4, 28011.

[87]. Yang G; Wang J; Li L; Ding S; Zhou S, Macromol. Biosci 2014, 14, 965. [PubMed: 24634305]

[88]. Yu Y; Kong L; Li L; Li N; Yan P, Nanoscale Research Letters 2015, 10, 343.

[89]. Yuan Z; Pan Y; Cheng R; Sheng L; Wu W; Pan G; Feng Q; Cui W, Nanotechnology 2016, 27, 245101. [PubMed: 27172065]

[90]. Yuan Z; Wu W; Zhang Z; Sun Z; Cheng R; Pan G; Wang X; Cui W, Colloids Surf., B 2017, 158, 363.

[91]. Zheng F; Wang S; Shen M; Zhu M; Shi X, Polym Chem 2013, 4, 933.

[92]. Zhou X; Chen L; Wang W; Jia Y; Chang A; Mo X; Wang H; He C, RSC Advances 2015, 5, 65897.

[93]. Hou Z; Li C; Ma P. a.; Cheng Z; Li X; Zhang X; Dai Y; Yang D; Lian H; Lin J, Adv. Funct. Mater 2012, 22, 2713.

[94]. Chen Y; Liu S; Hou Z; Ma P; Yang D; Li C; Lin J, Nano Res 2015, 8, 1917.

[95]. Jassal M; Sengupta S; Bhowmick S, Journal of Biomaterials Science, Polymer Edition 2015, 26, 1425. [PubMed: 26406285]

[96]. Jiang J; Xie J; Ma B; Bartlett DE; Xu A; Wang C-H, Acta Biomater 2014, 10, 1324. [PubMed: 24287161]

[97]. Yuan Z; Zhao X; Wang X; Qiu W; Chen X; Zheng Q; Cui W, International Journal of Clinical and Experimental Pathology 2014, 7, 5436. [PubMed: 25337186]

[98]. Liu H; Fu Y; Li Y; Ren Z; Li X; Han G; Mao C, Langmuir 2016, 32, 9083. [PubMed: 27557281]

[99]. a) Li X; Zhang Q; Ahmad Z; Huang J; Ren Z; Weng W; Han G; Mao C, J. Mater. Chem. B 2015, 3, 7449; [PubMed: 27398215] b) Zhang Q; Li X; Ren Z; Han G; Mao C, Eur. J. Inorg. Chem 2015, 4532; [PubMed: 27818612] c) Zhang Q; Li Y; Ren Z; Ahmad Z; Li X; Han G, Mater. Lett 2015, 152, 82;d) Li X; Li Y; Chen X; Li B; Gao B; Ren Z; Han G; Mao C, Langmuir 2016, 32, 3226. [PubMed: 27010624]

[100]. Xia Z; Fu Y; Gu T; Li Y; Liu H; Ren Z; Li X; Han G, Mater. Des 2017, 119, 85.

[101]. Breasted JH, The Edwin Smith Surgical Papyrus: hieroglyphic transliteration, translation and commentary Chic. UP: 1930; Vol. 1.

[102]. Svaasand LO; Gomer CJ; Morinelli E, Lasers in Medical Science 1990, 5, 121.

[103]. Huang X; Jain PK; El-Sayed IH; El-Sayed MA, Lasers in medical science 2008, 23, 217. [PubMed: 17674122]

[104]. Yang H-W; Hua M-Y; Hwang T-L; Lin K-J; Huang C-Y; Tsai R-Y; Ma C-CM; Hsu P-H; Wey S-P; Hsu P-W; Chen P-Y; Huang Y-C; Lu Y-J; Yen T-C; Feng L-Y; Lin C-W; Liu H-L; Wei K-C, Adv. Mater 2013, 25, 3605. [PubMed: 23712913]

[105]. Lee J; Lee D; Cho SJ; Seo J-H; Liu D; Eom C-B; Ma Z, Appl. Phys. Lett 2017, 111, 063110.

[106]. Shi H; Liu T; Fu C; Li L; Tan L; Wang J; Ren X; Ren J; Wang J; Meng X, Biomaterials 2015, 44, 91. [PubMed: 25617129]

[107]. Vittorino E; Sciortino MT; Siracusano G; Sortino S, ChemMedChem 2011, 6, 1551. [PubMed: 21661112]

[108]. a) Cheng L; Wang C; Feng L; Yang K; Liu Z, Chem. Rev 2014, 114, 10869; [PubMed: 25260098] b) Chen Q; Wen J; Li H; Xu Y; Liu F; Sun S, Biomaterials 2016, 106, 144; [PubMed: 27561885] c) Chen Y-W; Su Y-L; Hu S-H; Chen S-Y, Adv. Drug Delivery Rev 2016, 105, 190.

[109]. Liang C; Xu L; Song G; Liu Z, Chem. Soc. Rev 2016, 45, 6250. [PubMed: 27333329]

[110]. a) Zhang Z; Wang J; Chen C, Adv. Mater 2013, 25, 3869; [PubMed: 24048973] b) Huang H-C; Barua S; Sharma G; Dey SK; Rege K, J. Controlled Release 2011, 155, 344;c) Song X; Chen Q; Liu Z, Nano Res 2015, 8, 340.

[111]. a) Yang X; Yang M; Pang B; Vara M; Xia Y, Chem. Rev 2015, 115, 10410; [PubMed: 26293344] b) Alkilany AM; Thompson LB; Boulos SP; Sisco PN; Murphy CJ, Adv. Drug Delivery Rev 2012, 64, 190;c) Dykman L; Khlebtsov N, Chem. Soc. Rev 2012, 41, 2256; [PubMed: 22130549] d) Qiu P; Yang M; Qu X; Huai Y; Zhu Y; Mao C, Biomaterials 2016, 104, 138; [PubMed: 27449950] e) Qu X; Qiu P; Zhu Y; Yang M; Mao C, Npg Asia Materials 2017, 9, e452. [PubMed: 29657602]

[112]. a) Wang S; Shang L; Li L; Yu Y; Chi C; Wang K; Zhang J; Shi R; Shen H; Waterhouse GIN; Liu S; Tian J; Zhang T; Liu H, Adv. Mater 2016, 28, 8379; [PubMed: 27461987] b) Wang G; Zhang F; Tian R; Zhang L; Fu G; Yang L; Zhu L, ACS Appl. Mater. Interfaces 2016, 8, 5608; [PubMed: 26860184] c) Tu X; Wang L; Cao Y; Ma Y; Shen H; Zhang M; Zhang Z, Carbon 2016, 97, 35;d) Li Y; Fu Y; Ren Z; Li X; Mao C; Han G, J. Mater. Chem. B 2017, 5, 7504. [PubMed: 29255606]

[113]. a) Chen Z; Wang Q; Wang H; Zhang L; Song G; Song L; Hu J; Wang H; Liu J; Zhu M; Zhao D, Adv. Mater 2013, 25, 2095; [PubMed: 23427112] b) Liu T; Shi S; Liang C; Shen S; Cheng L; Wang C; Song X; Goel S; Barnhart TE; Cai W; Liu Z, ACS Nano 2015, 9, 950; [PubMed: 25562533] c) Meng Z; Wei F; Wang R; Xia M; Chen Z; Wang H; Zhu M, Adv. Mater 2016, 28, 245; [PubMed: 26551334] d) Wu Z-C; Li W-P; Luo C-H; Su C-H; Yeh C-S, Adv. Funct. Mater 2015, 25, 6527;e) Li L; Lu Y; Jiang C; Zhu Y; Yang X; Hu X; Lin Z; Zhang Y; Peng M; Xia H; Mao C, Adv. Funct. Mater 2018, 28, 1704623. [PubMed: 29706855]

[114]. a) You Q; Sun Q; Wang J; Tan X; Pang X; Liu L; Yu M; Tan F; Li N, Nanoscale 2017, 9, 3784; [PubMed: 28067380] b) Su S; Ding Y; Li Y; Wu Y; Nie G, Biomaterials 2016, 80, 169; [PubMed: 26708642] c) Yang Z; Ren J; Ye Z; Zhu W; Xiao L; Zhang L; He Q; Xu Z; Xu H, J. Mater. Chem. B 2017, 5, 1108.

[115]. Cheng M; Wang H; Zhang Z; Li N; Fang X; Xu S, ACS Appl. Mater. Interfaces 2014, 6, 1569. [PubMed: 24432724]

[116]. Chen Y; Li C; Hou Z; Huang S; Liu B; He F; Luo L; Lin J, New J Chem 2015, 39, 4987.

[117]. Mauro N; Scialabba C; Pitarresi G; Giammona G, Int. J. Pharm 2017, 526, 167. [PubMed: 28442269]

[118]. Wang X; Lv F; Li T; Han Y; Yi Z; Liu M; Chang J; Wu C, ACS Nano 2017, 11, 11337. [PubMed: 29059516]

[119]. Gong L; Yan L; Zhou R; Xie J; Wu W; Gu Z, J. Mater. Chem. B 2017, 5, 1873.

[120]. Lin Z; Liu Y; Ma X; Hu S; Zhang J; Wu Q; Ye W; Zhu S; Yang D; Qu D; Jiang J, Scientific Reports 2015, 5.

[121]. Fisher JW; Sarkar S; Buchanan CF; Szot CS; Whitney J; Hatcher HC; Torti SV; Rylander CG; Rylander MN, Cancer Res 2010, 70, 9855. [PubMed: 21098701]

[122]. Yang T-I; Chang S-H, Nanotechnology 2017, 28, 055601. [PubMed: 28008893]

[123]. Ma M; Wu Y; Zhou J; Sun Y; Zhang Y; Gu N, J. Magn. Magn. Mater 2004, 268, 33.

[124]. a) Yoo D; Jeong H; Noh SH; Lee JH; Cheon J, Angew. Chem. Int. Ed 2013, 52, 13047;b) Canfarotta F; Piletsky SA, Advanced Healthcare Materials 2014, 3, 160. [PubMed: 24497448]

[125]. Lin T-C; Lin F-H; Lin J-C, Acta Biomater 2012, 8, 2704. [PubMed: 22484694]

[126]. Lin T-C; Lin F-H; Lin J-C, Journal of Biomaterials Science, Polymer Edition 2013, 24, 1152. [PubMed: 23683044]

[127]. Huang C; Soenen SJ; Rejman J; Trekker J; Chengxun L; Lagae L; Ceelen W; Wilhelm C; Demeester J; De Smedt SC, Adv. Funct. Mater 2012, 22, 2479.

[128]. a) Hu J; Tang Y. a.; Elmenoufy AH; Xu H; Cheng Z; Yang X, Small 2015, 11, 5860; [PubMed: 26398119] b) Obaid G; Broekgaarden M; Bulin A-L; Huang H-C; Kuriakose J; Liu J; Hasan T, Nanoscale 2016, 8, 12471; [PubMed: 27328309] c) Fan W; Huang P; Chen X, Chem. Soc. Rev 2016, 45, 6488; [PubMed: 27722560] d) Shanmugam V; Selvakumar S; Yeh C-S, Chem. Soc. Rev 2014, 43, 6254; [PubMed: 24811160] e) Gandra N; Abbineni G; Qu X; Huai Y; Wang L; Mao C, Small 2013, 9, 215; [PubMed: 23047655] f) Kalarical Janardhanan S; Narayan S; Abbineni G; Hayhurst A; Mao C, Mol. Cancer Ther 2010, 9, 2524. [PubMed: 20807781]

[129]. Brown JE; Brown SB; Vernon DI, Journal of the Society of Dyers and Colourists 1999, 115, 249.

[130]. Lin L; Xiong L; Wen Y; Lei S; Deng X; Liu Z; Chen W; Miao X, J. Biomed. Nanotechnol 2015, 11, 531. [PubMed: 26310063]

[131]. Severyukhina AN; Petrova NV; Smuda K; Terentyuk GS; Klebtsov BN; Georgieva R; Bäumler H; Gorin DA, Colloids Surf., B 2016, 144, 57.

[132]. a) Lim KS; Oh KW; Kim SH, Polym. Int 2012, 61, 1519;b) Osifeko OL; Nyokong T, Dyes and Pigments 2014, 111, 8.

[133]. Gmurek M; Bizukojć M; Mosinger J; Ledakowicz S, Catal. Today 2015, 240, 160.

[134]. Henke P; Lang K; Kubát P; Sýkora J; Šlouf M; Mosinger J, ACS Appl. Mater. Interfaces 2013, 5, 3776. [PubMed: 23566280]

[135]. El-Khordagui L; El-Sayed N; Galal S; El-Gowelli H; Omar H; Mohamed M, Int. J. Pharm 2017, 520, 139. [PubMed: 28163229]

[136]. Yuan Y; Feng G; Qin W; Tang BZ; Liu B, Chem. Commun 2014, 50, 8757.

[137]. a) Yan L; Chang Y-N; Yin W; Tian G; Zhou L; Liu X; Xing G; Zhao L; Gu Z; Zhao Y, Biomaterials Science 2014, 2, 1412;b) Fan W; Yung B; Huang P; Chen X, Chem. Rev 2017, 117, 13566. [PubMed: 29048884]

[138]. a) DeRosa MC; Crutchley RJ, Coord. Chem. Rev 2002, 233–234, 351;b) van Dongen GAMS; Visser GWM; Vrouenraets MB, Adv. Drug Delivery Rev 2004, 56, 31.

[139]. a) Redmond RW; Kochevar IE, Photochem. Photobiol 2006, 82, 1178; [PubMed: 16740059] b) Baier A; Maier M; Engl R; Landthaler M; Baumler W, J. Phys. Chem. B 2005, 109, 3041; [PubMed: 16851318] c) Snyder JW; Skovsen E; Lambert JDC; Poulsen L; Ogilby PR, Phys. Chem. Chem. Phys 2006, 8, 4280. [PubMed: 16986070]

[140]. Moan J; Berg K, Photochem. Photobiol 1991, 53, 549. [PubMed: 1830395]

[141]. a) Somia N; Verma IM, Nat. Rev. Genet 2000, 1, 91; [PubMed: 11253666] b) Verma IM; Weitzman MD, Annu. Rev. Biochem 2005, 74, 711; [PubMed: 15952901] c) Viiala NO; Larsen SR; Rasko JEJ, Seminars in Thrombosis and Hemostasis 2009, 35, 81; [PubMed: 19308896] d) Zhou Z; Liu X; Zhu D; Wang Y; Zhang Z; Zhou X; Qiu N; Chen X; Shen Y, Adv. Drug Delivery Rev 2017, 115, 115.

[142]. Kim J; Kim J; Jeong C; Kim WJ, Adv. Drug Delivery Rev 2016, 98, 99.

[143]. a) Teo PY; Cheng W; Hedrick JL; Yang YY, Adv. Drug Delivery Rev 2016, 98, 41;b) Kay MA, Nature Reviews Genetics 2011, 12, 316.

[144]. Achille C; Sundaresh S; Chu B; Hadjiargyrou M, PLOS ONE 2012, 7, e52356. [PubMed: 23285007]

[145]. a) Gottesman MM; Fojo T; Bates SE, Nature Reviews Cancer 2002, 2, 48; [PubMed: 11902585] b) Szakacs G; Paterson JK; Ludwig JA; Booth-Genthe C; Gottesman MM, Nature Reviews Drug Discovery 2006, 5, 219. [PubMed: 16518375]

[146]. a) Liu J; Wang C; Wang X; Wang X; Cheng L; Li Y; Liu Z, Adv. Funct. Mater 2015, 25, 384;b) Sun X; Wang C; Gao M; Hu A; Liu Z, Adv. Funct. Mater 2015, 25, 2386.

[147]. Feng L; Li K; Shi X; Gao M; Liu J; Liu Z, Advanced Healthcare Materials 2014, 3, 1261. [PubMed: 24652715]

[148]. Zhang Z; Liu S; Xiong H; Jing X; Xie Z; Chen X; Huang Y, Acta Biomater 2015, 26, 115. [PubMed: 26260417]

[149]. Chen Y; Hou Z; Liu B; Huang S; Li C; Lin J, Dalton Trans 2015, 44, 3118. [PubMed: 25567415]

[150]. a) Hu SH; Liao BJ; Chiang CS; Chen PJ; Chen IW; Chen SY, Adv. Mater 2012, 24, 3627; [PubMed: 22689346] b) Li T-J; Huang C-C; Ruan P-W; Chuang K-Y; Huang K-J; Shieh D-B; Yeh C-S, Biomaterials 2013, 34, 7873. [PubMed: 23876757]

[151]. GhavamiNejad A; Sasikala ARK; Unnithan AR; Thomas RG; Jeong YY; Vatankhah-Varnoosfaderani M; Stadler FJ; Park CH; Kim CS, Adv. Funct. Mater 2015, 25, 2867.

[152]. Sasikala ARK; Unnithan AR; Yun Y-H; Park CH; Kim CS, Acta Biomater 2016, 31, 122. [PubMed: 26687978]

[153]. Kim YJ; Ebara M; Aoyagi T, Adv. Funct. Mater 2013, 23, 5753.

[154]. Sun T-M; Du J-Z; Yao Y-D; Mao C-Q; Dou S; Huang S-Y; Zhang P-Z; Leong KW; Song E-W; Wang J, ACS Nano 2011, 5, 1483. [PubMed: 21204585]

[155]. Taheri M; Mahjoubi F, Dis. Markers 2013, 34.

[156]. Beh CW; Seow WY; Wang Y; Zhang Y; Ong ZY; Ee PLR; Yang Y-Y, Biomacromolecules 2009, 10, 41. [PubMed: 19072631]

[157]. a) Wang Y; Gao S; Ye W-H; Yoon HS; Yang Y-Y, Nat. Mater 2006, 5, 791; [PubMed: 16998471] b) Yang B; Dong X; Lei Q; Zhuo R; Feng J; Zhang X, ACS Appl. Mater. Interfaces 2015, 7, 22084. [PubMed: 26398113]

[158]. Sukumar UK; Packirisamy G, ACS Appl. Mater. Interfaces 2015, 7, 18717. [PubMed: 26234345]

[159]. Che H-L; Lee HJ; Uto K; Ebara M; Kim WJ; Aoyagi T; Park I-K, Journal of nanoscience and nanotechnology 2015, 15, 7971. [PubMed: 26726449]

[160]. Lei C; Cui Y; Zheng L; Kah-Hoe Chow P; Wang C-H, Biomaterials 2013, 34, 7483. [PubMed: 23820014]

[161]. Lucky SS; Soo KC; Zhang Y, Chem. Rev 2015, 115, 1990. [PubMed: 25602130]

[162]. a) Bhana S; Lin G; Wang L; Starring H; Mishra SR; Liu G; Huang X, ACS Appl. Mater. Interfaces 2015, 7, 11637; [PubMed: 25965727] b) Song CW; Park HJ; Lee CK; Griffin R, International Journal of Hyperthermia 2005, 21, 761. [PubMed: 16338859]

[163]. Fu Y; Liu H; Ren Z; Li X; Huang J; Best S; Han G, J. Mater. Chem. B 2017, 5, 5128.

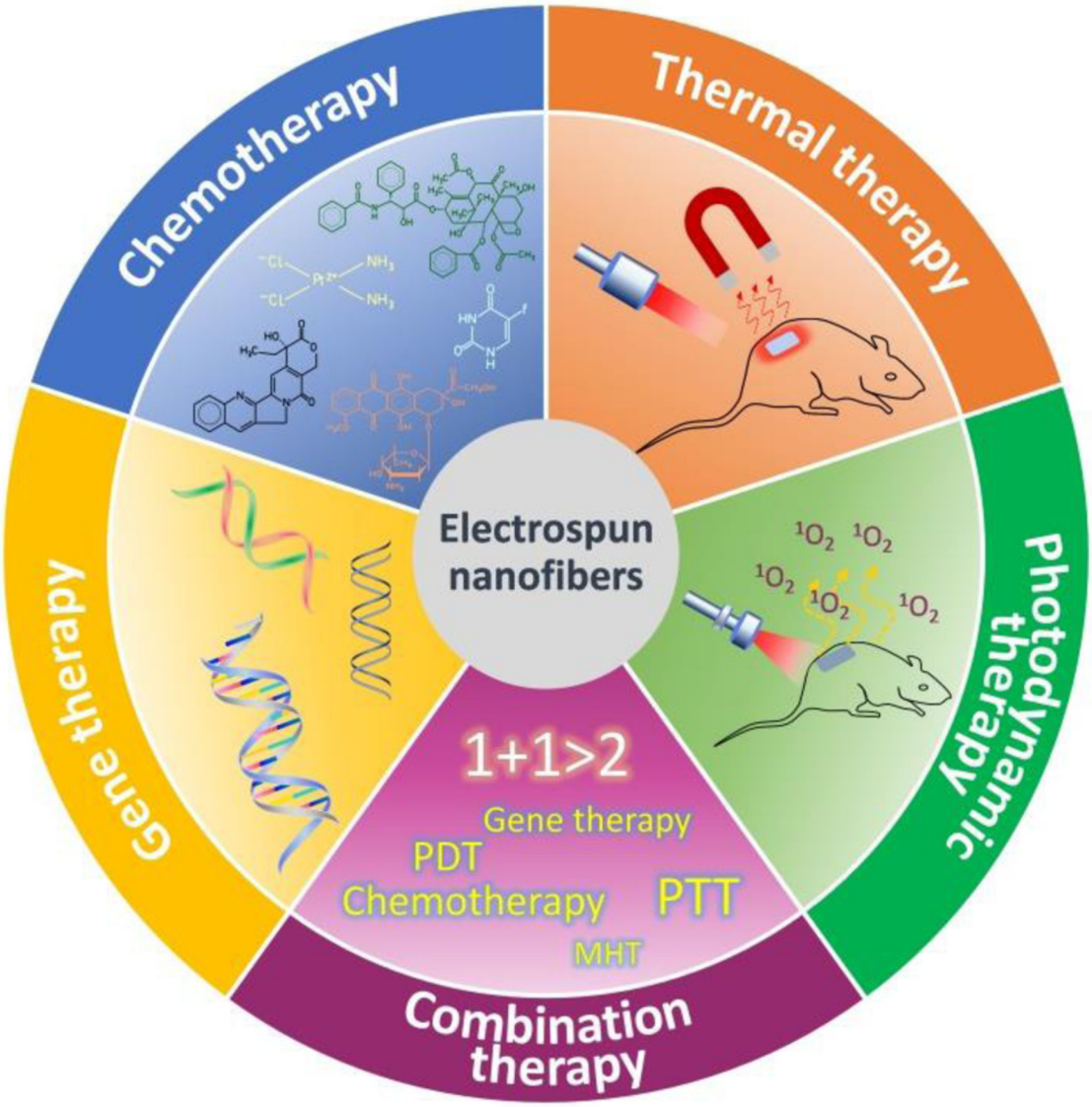

Figure 1.
The applications of electrospun nanofibers in cancer therapy.

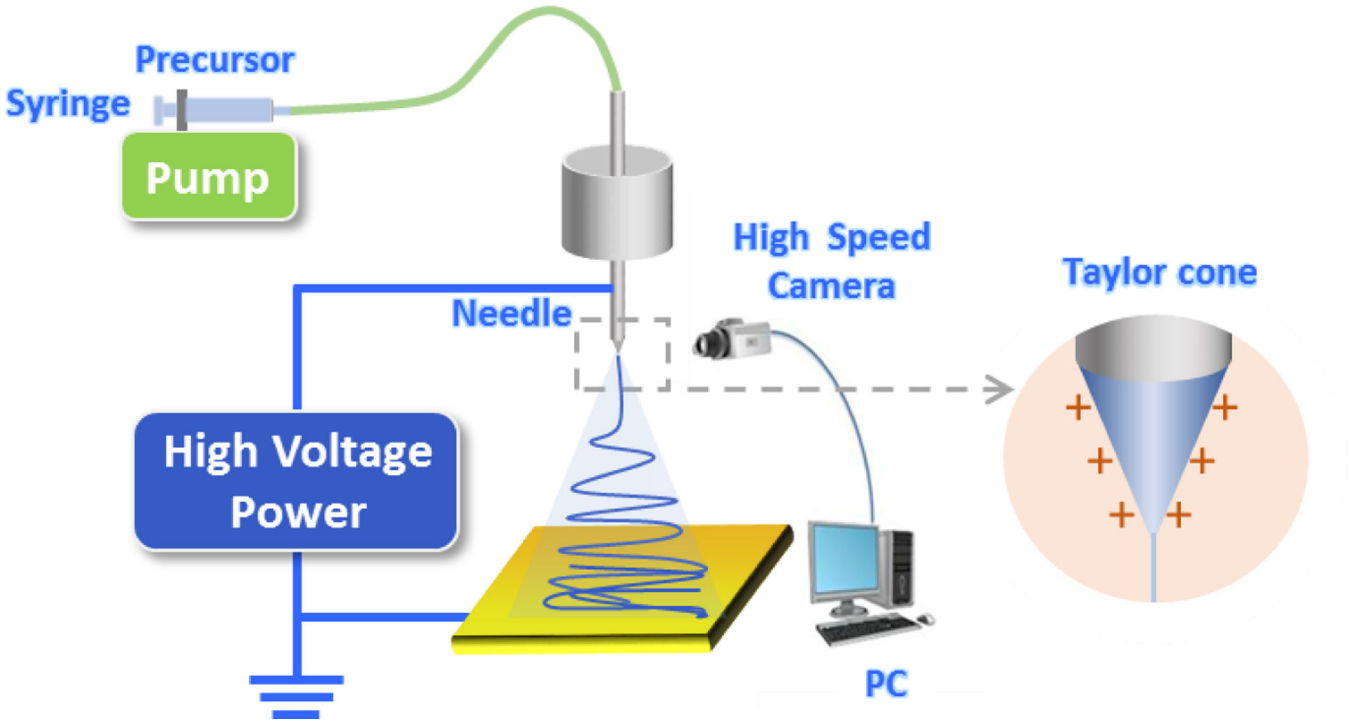

Figure 2.
The typical schematic diagram of electrospinning process.

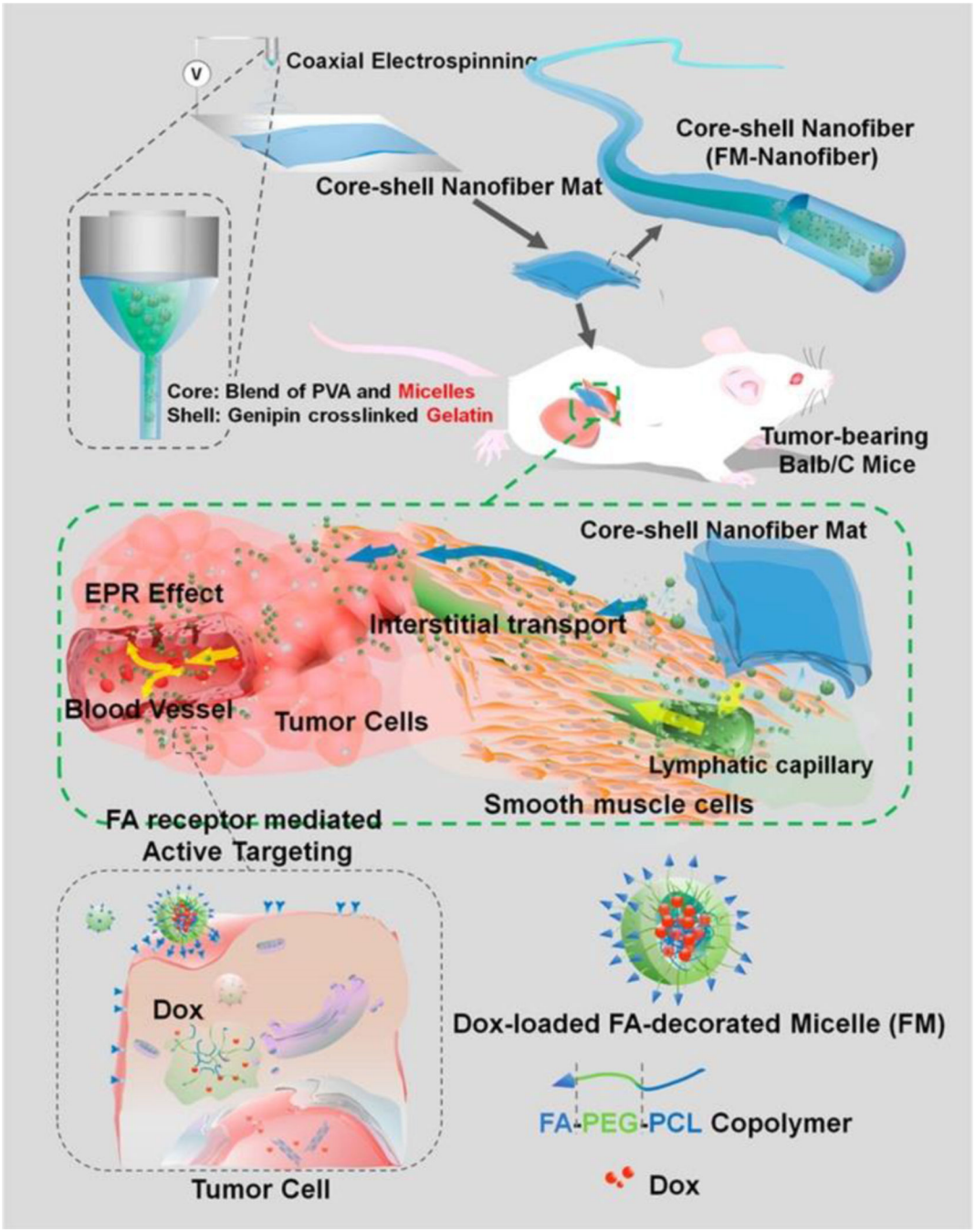

Figure 3.

The implantable DOX loaded micelle-in-nanofiber platform synthesized by coaxial electrospinning.

Reproduced with permission.[62] Copyright 2015, American Chemical Society.

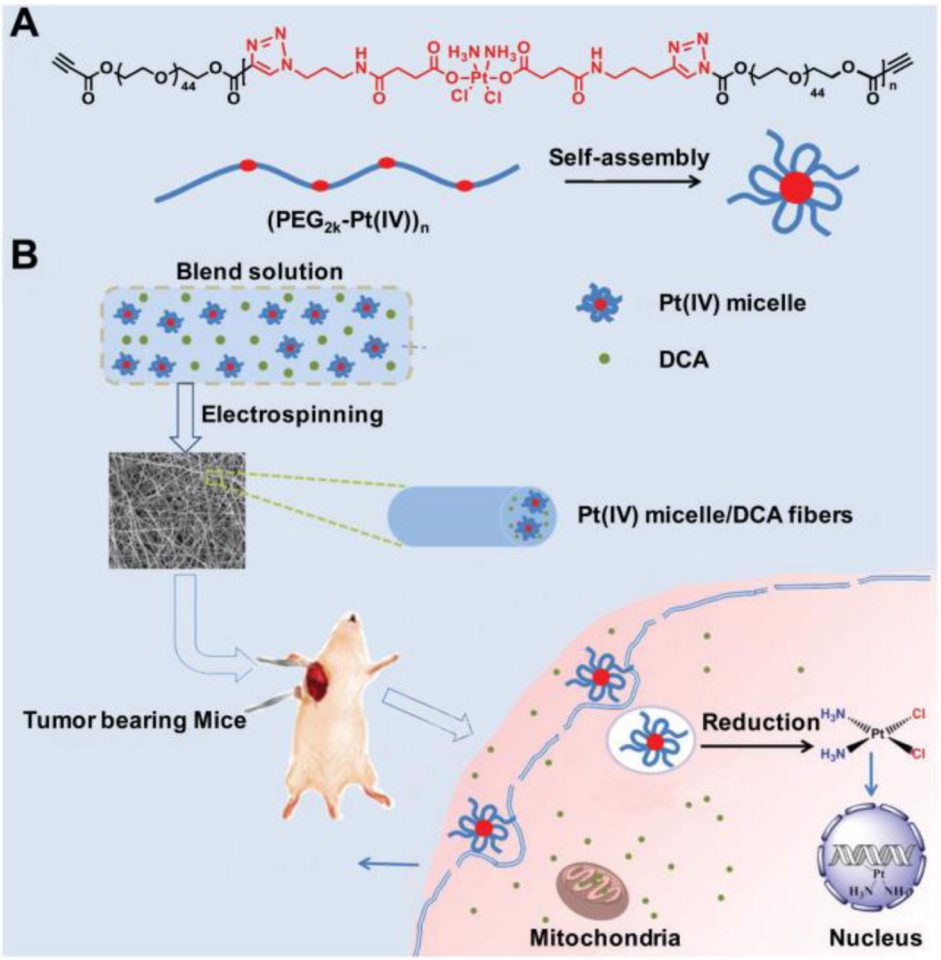

Figure 4.

(A) The formation process of $Pt(_{IV})$ micelle; (B) the synthesis and local therapy of micelle-incoparated fibers.

Reproduced with permission.[64] Copyright 2017, Royal Society of Chemistry.

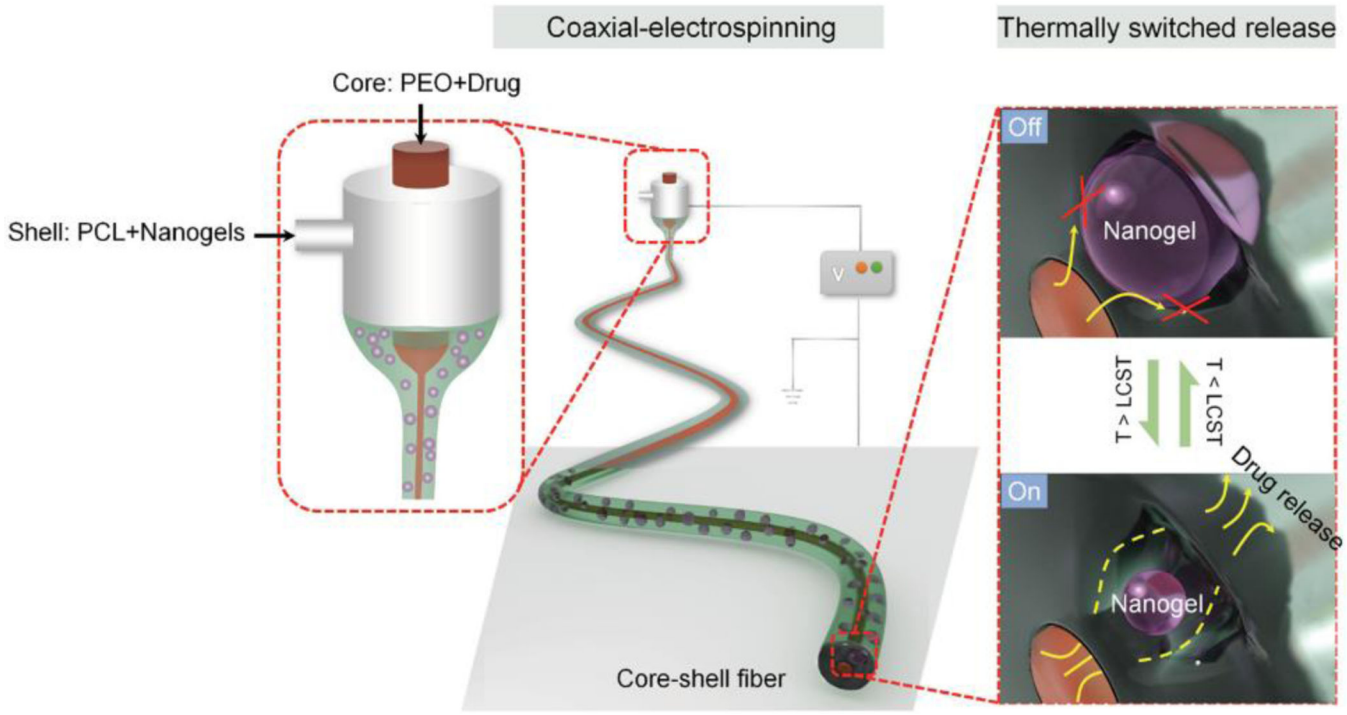

Figure 5.

Schematic illustration of the thermal responsive nanogel-in-microfiber drug delivery system. Reproduced with permission.[66] Copyright 2015, Wiley-VCH.

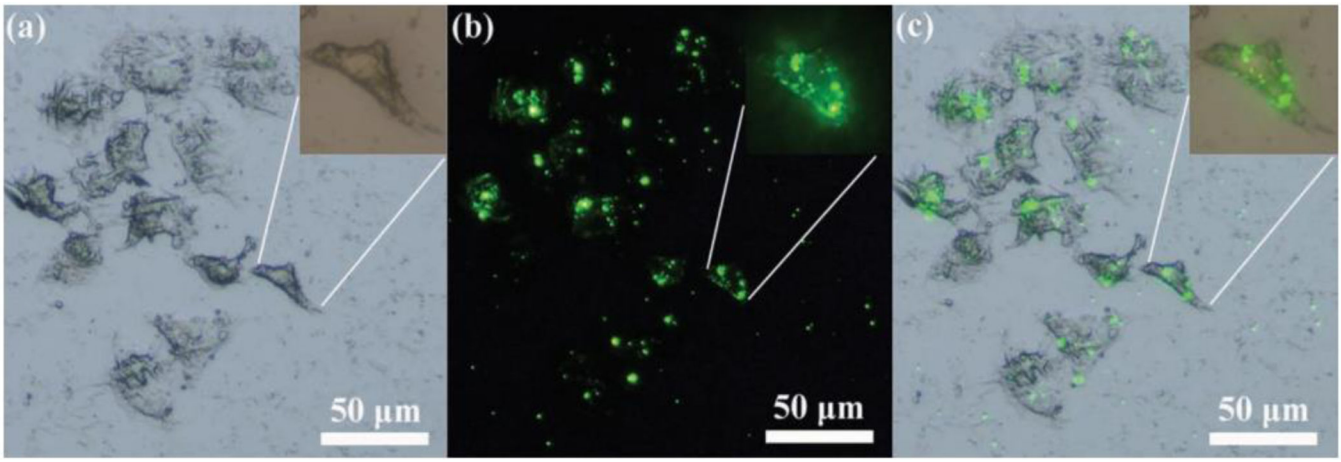

Figure 6.

(a) The bright-field image, (b) luminescent image and (c) the merged image of cancer cells incubated with upconversion luminescent composite nanofibers.

Reproduced with permission.[93] Copyright 2012, Wiley-VCH.

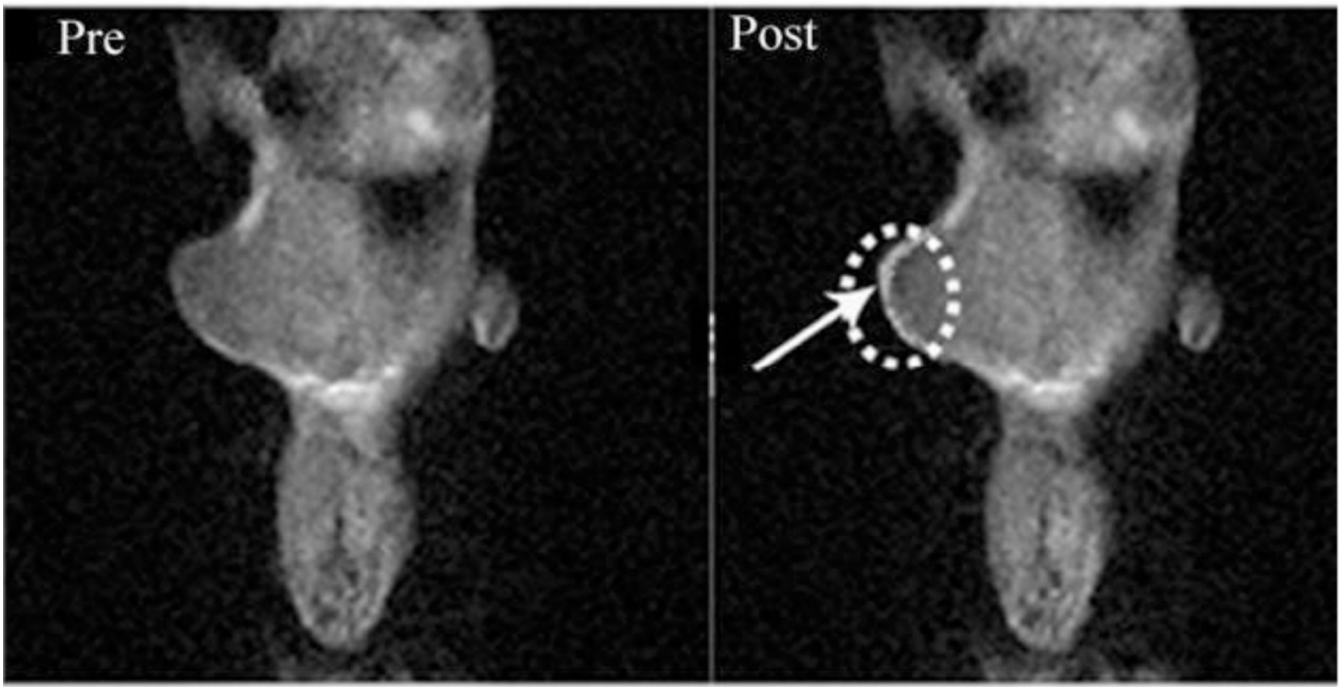

Figure 7.
MR images of tumor-bearing mice pre and post pasting the composite mesh. Reproduced with permission.[94] Copyright 2015, Springer-Verlag.

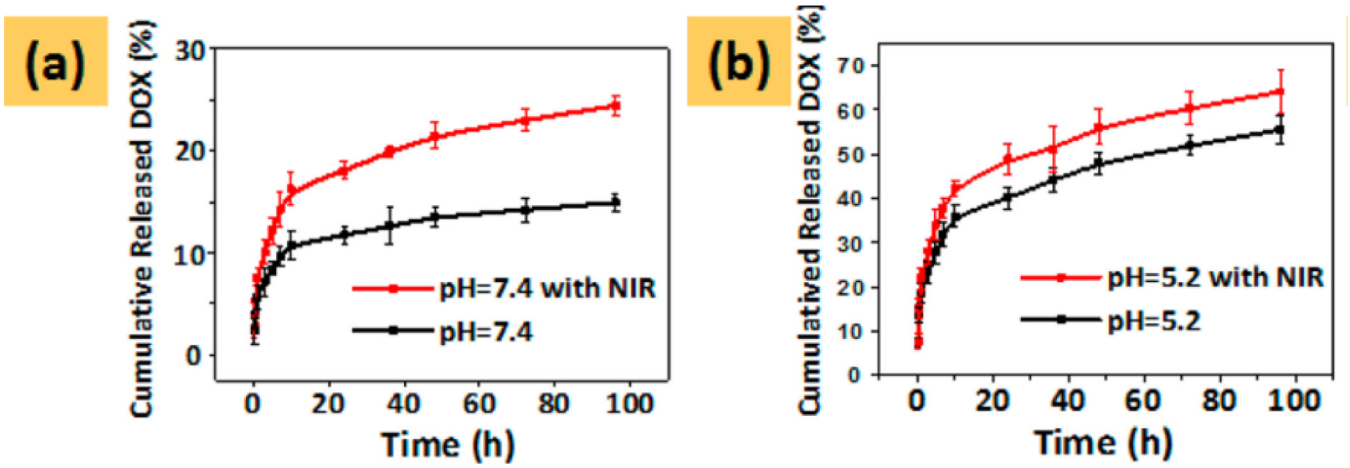

Figure 8.

The effect of NIR light on DOX release kinetics of CTO:Yb,Er-PAA nanofibers in different pH values.

Reproduced with permission.[98] Copyright 2016, American Chemical Society.

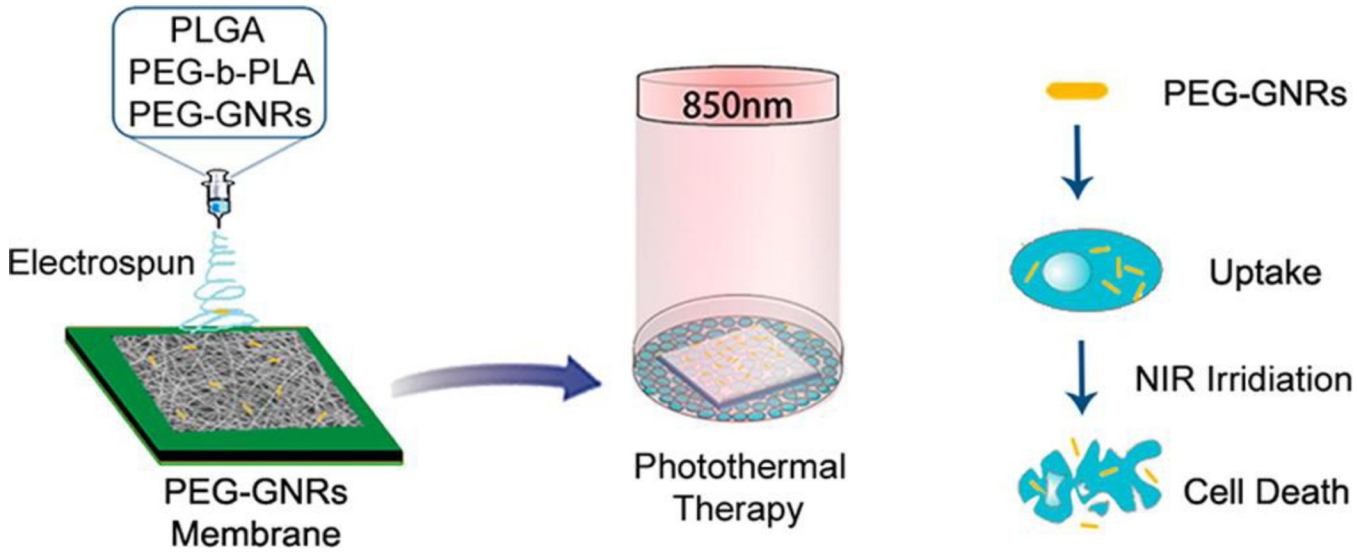

Figure 9.

PEG-GNRs-incorporated PLGA/ PLA-b-PEG fibrous membrane for *in vitro* photothermal therapy.

Reproduced with permission.[115] Copyright 2014, American Chemical Society.

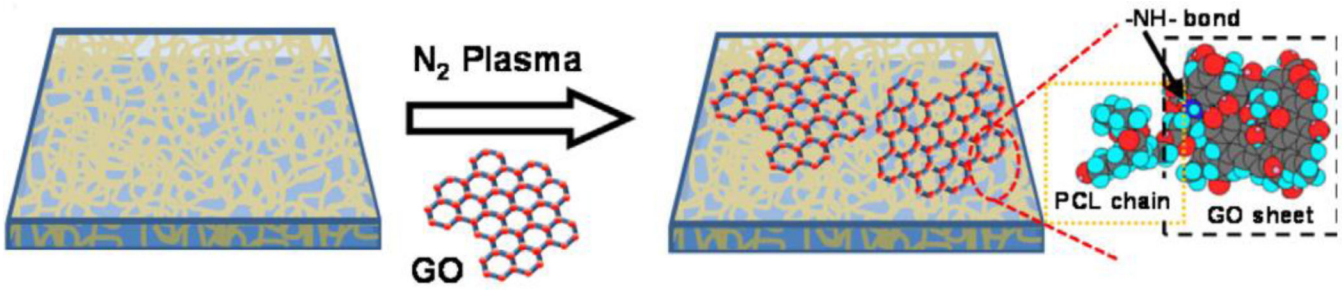

Figure 10.
The synthesis of PCL-GO composite nanofibers.
Reproduced with permission.[117] Copyright 2017, Elsevier.

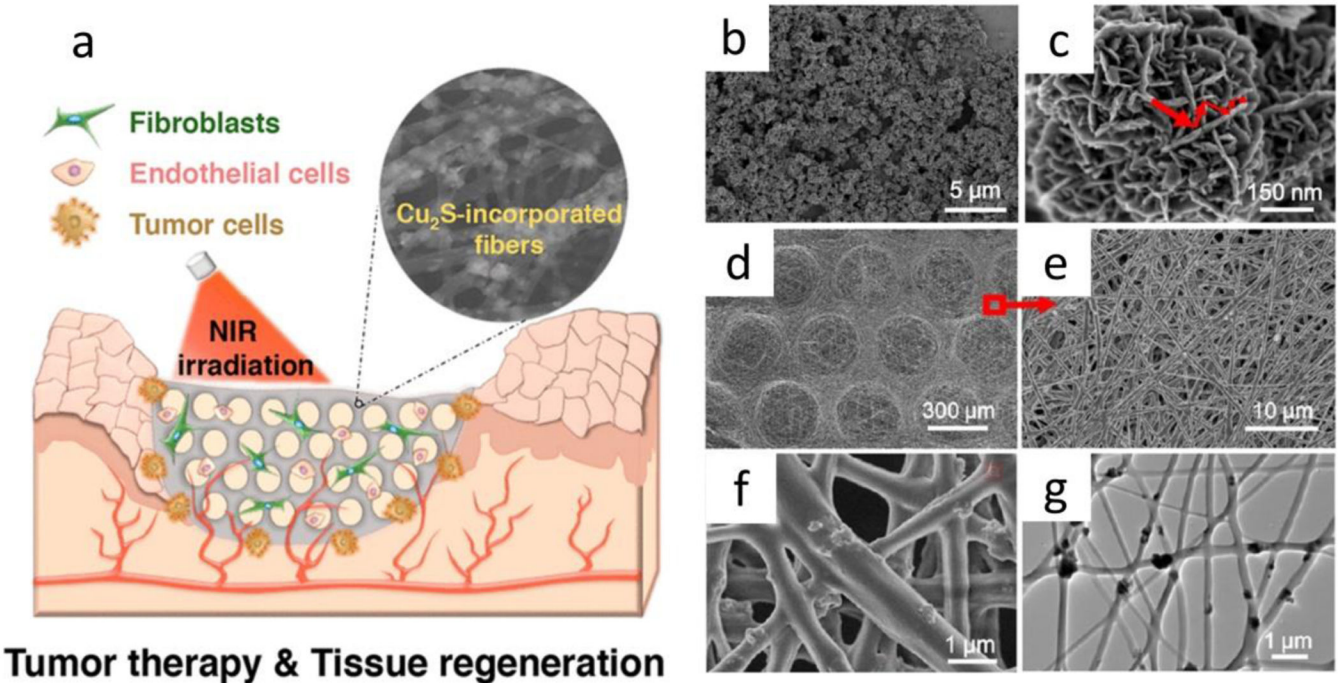

Figure 11.

(a) Cu_2S particles-incorporated fibers for tumor therapy and tissue regeneration, (b, c) SEM images of Cu_2S nanoparticles, (d, e, f) SEM images and (g) TEM image of micropatterned CS-PLA/PCL membranes with Cu_2S nanoflowers.

Reproduced with permission.[118] Copyright 2017, American Chemical Society.

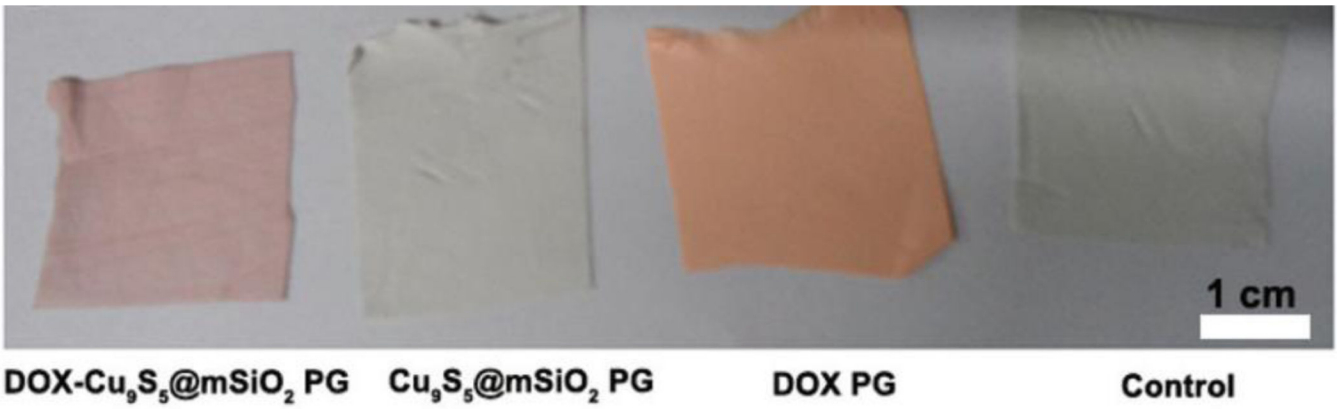

Figure 12.
The digital photographs of electrospun composite nanofibers.
Reproduced with permission.[149] Copyright 2015, Royal Society of Chemistry.

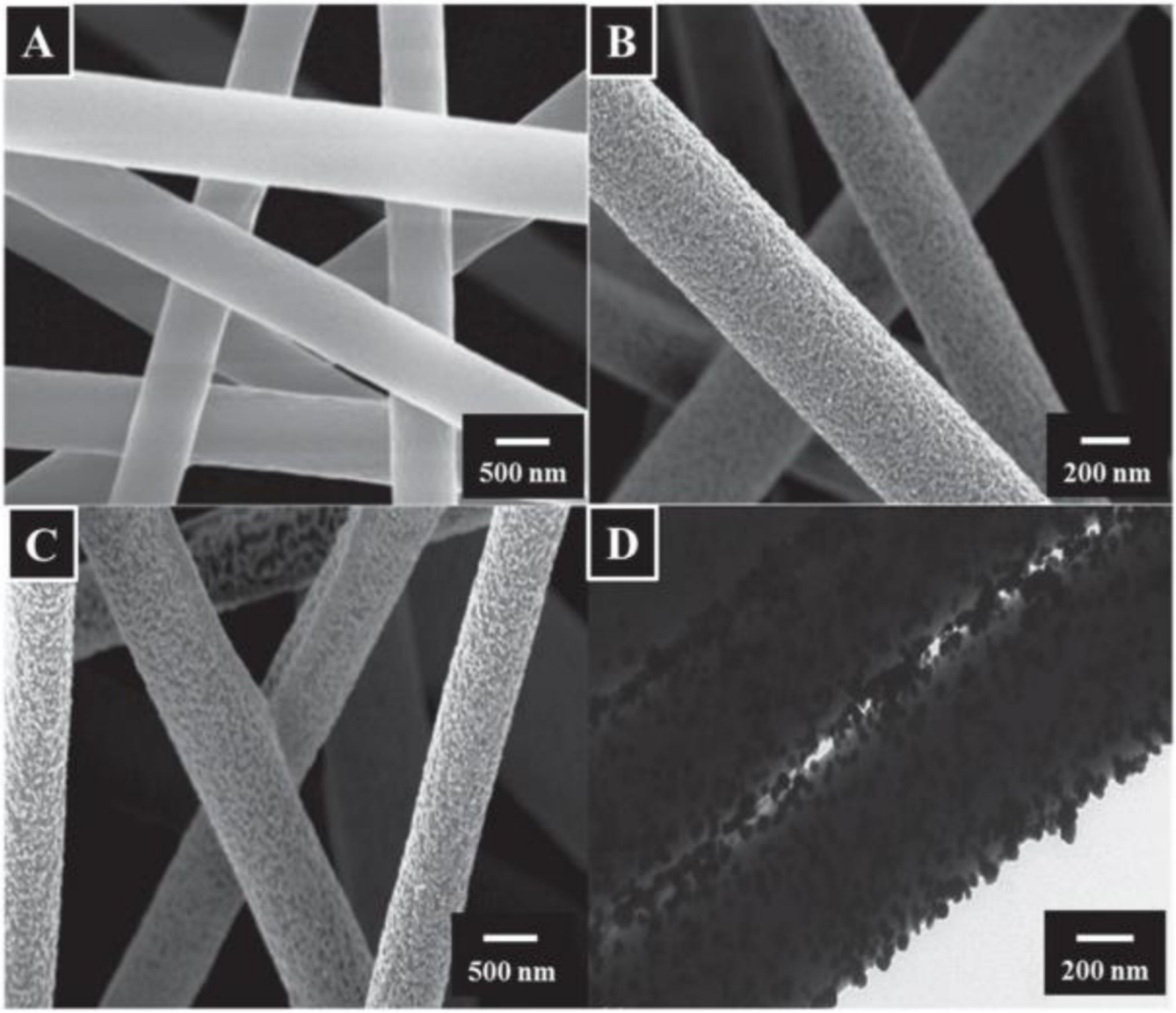

Figure 13.

SEM images of (A) MADO nanofibers, (B) MADO–Fe_3O_4 nanofibers and (C) MADO–Fe_3O_4–BTZ nanofibers; (D) TEM image of MADO–Fe_3O_4–BTZ nanofibers. Reproduced with permission.[151] Copyright 2015, Wiley-VCH.

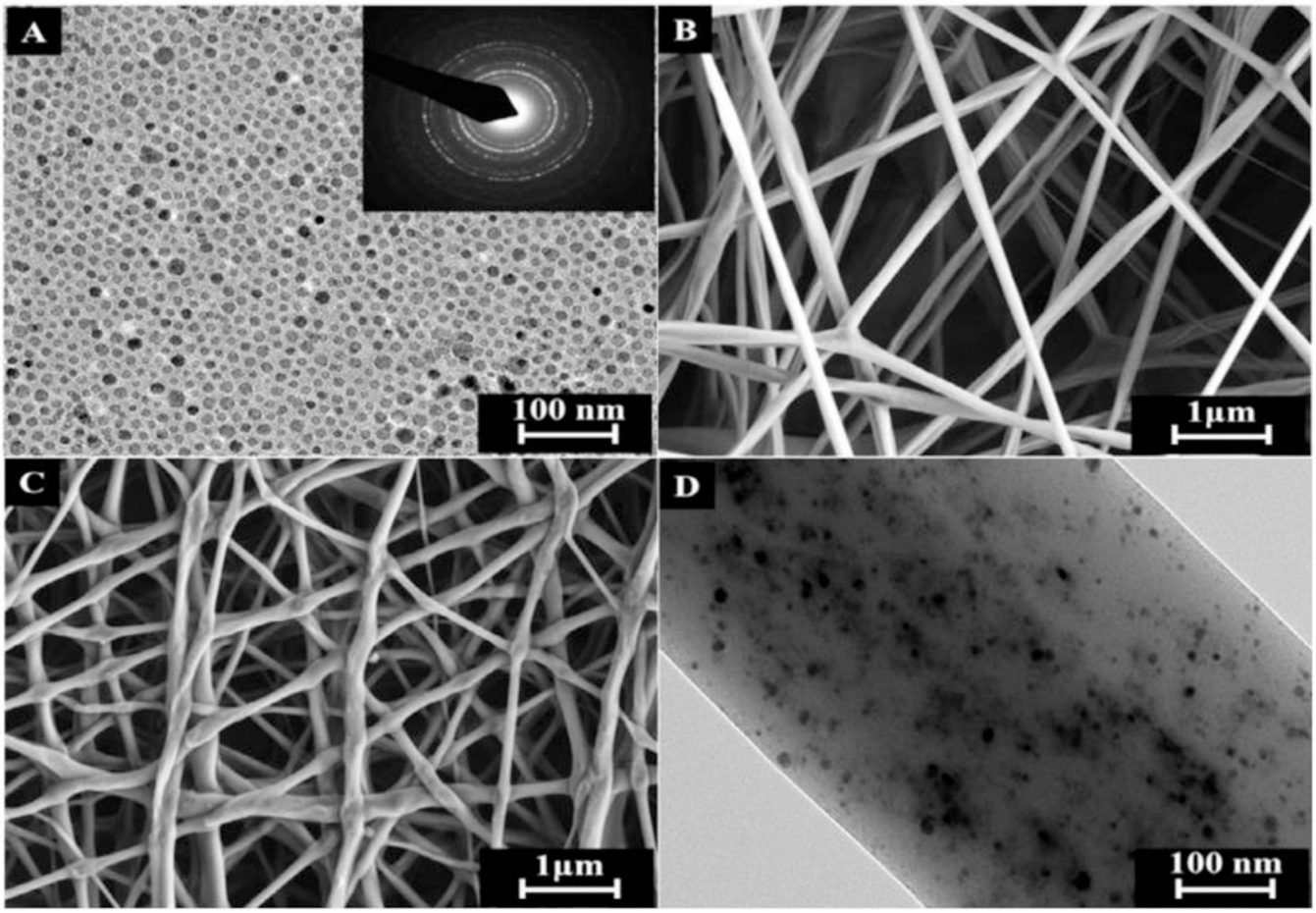

Figure 14.

(A) TEM image of IONPs (inset: SAED pattern), SEM image of (B) PLGA nanofibers and (C) MNF, (D) TEM image of MNF.

Reproduced with permission.[152] Copyright 2016, Elsevier.

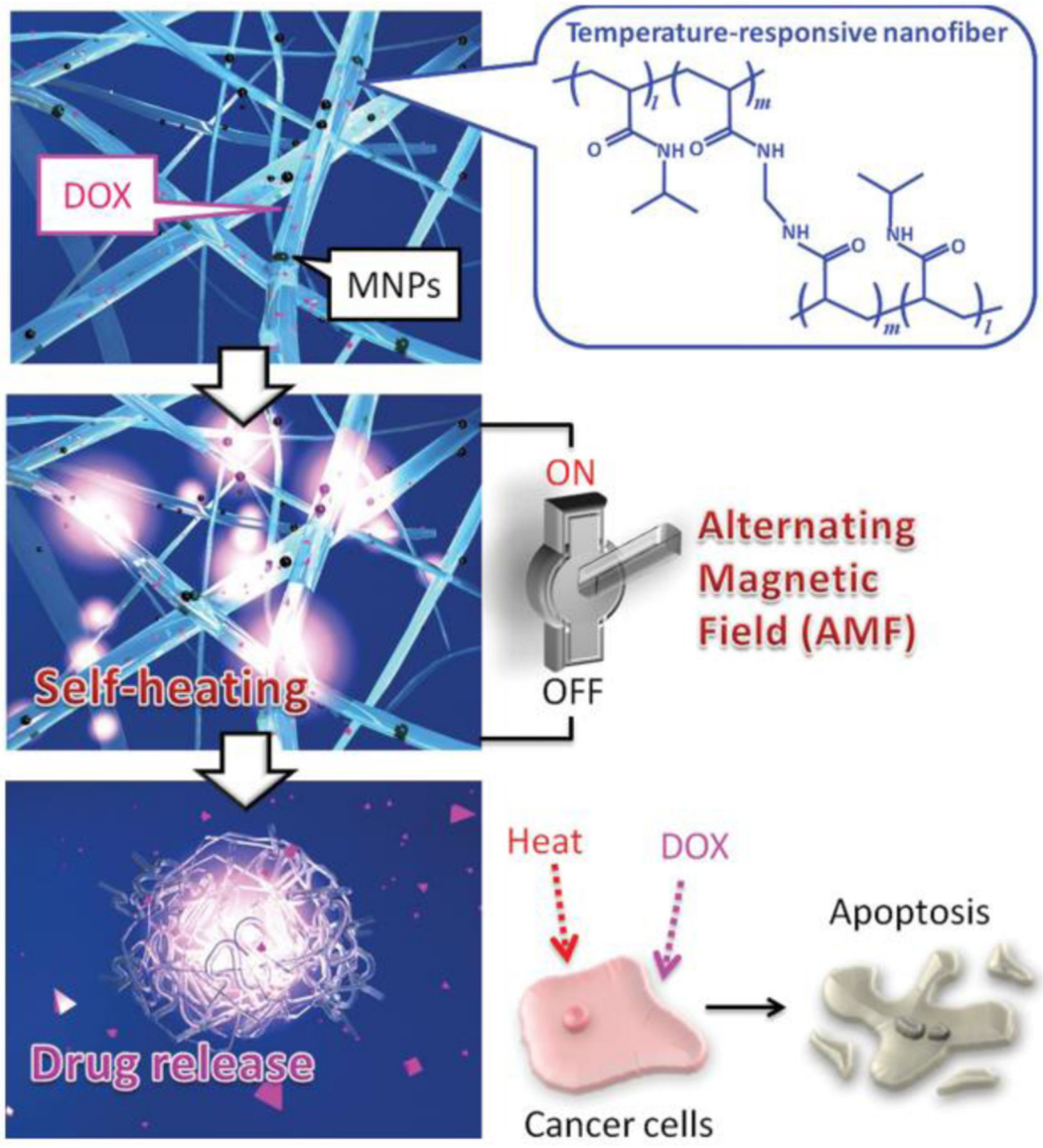

Figure 15.

Smart magnetic thermal platform based on MNPs/DOX/poly(NIPAAm-coHMAAm) nanofibers.

Reproduced with permission.[153] Copyright 2013, Wiley-VCH.

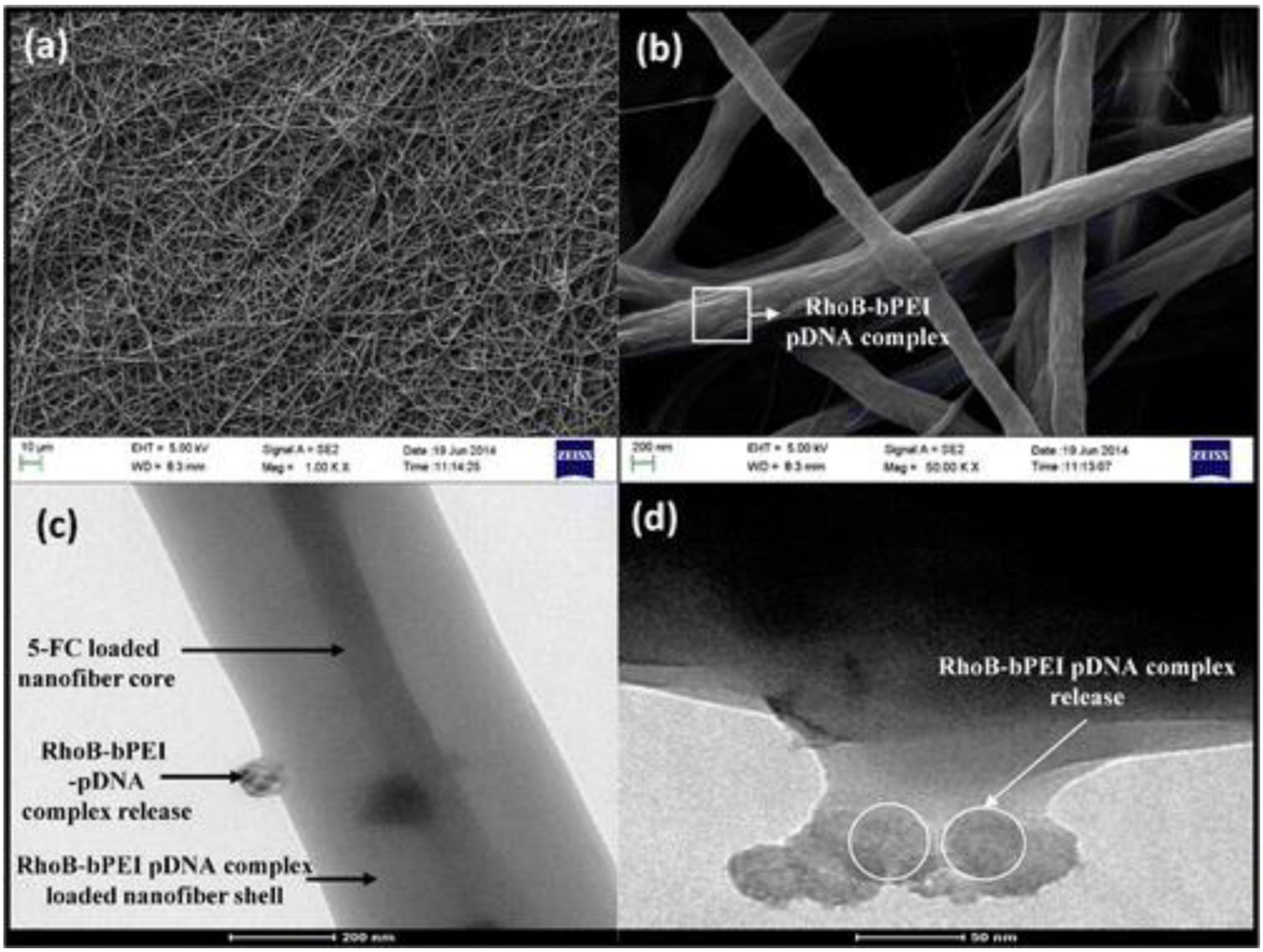

Figure 16.

(a, b) SEM images and (c, d) TEM images of RBP and 5-FC co-loaded core−shell nanofibers.

Reproduced with permission.[158] Copyright 2015, American Chemical Society.

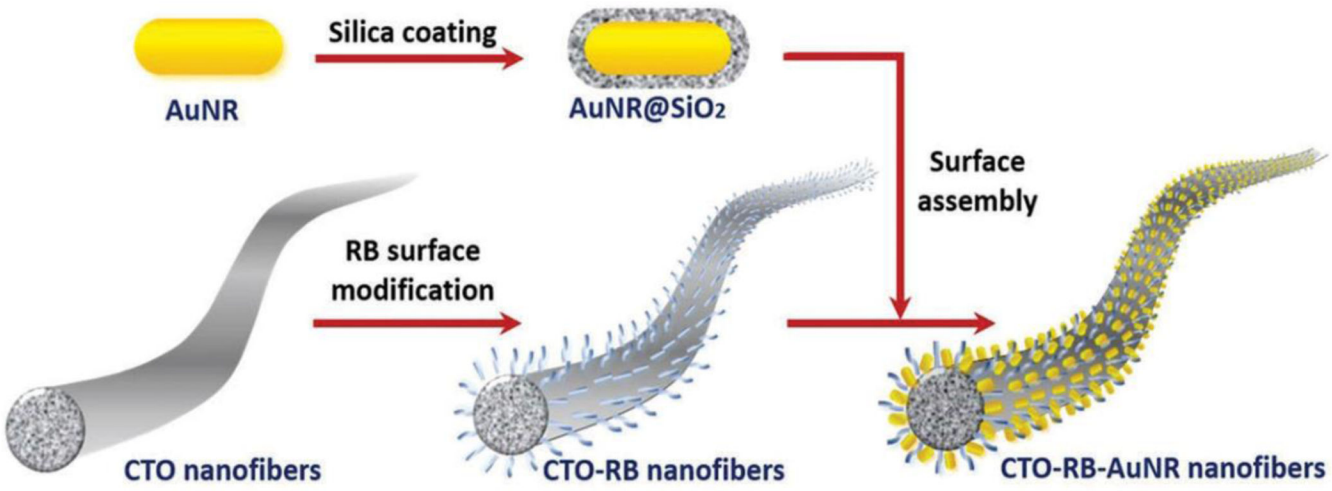

Figure 17.

Step-by-step synthesis of CTO–RB–AuNR composite nanofibers. Reproduced with permission.[163] Copyright 2017, Royal Society of Chemistry.

Table 1.

A summary of polymer nanofiber LDDSs for chemotherapy.

Delivery systems	Fiber diameter	Drug	Drug loading efficiency or content	Drug release mechanism	Drug release time	Cancer types	Ref
Poly(ε-caprolactone) (PCL)/ poly(glycerol monostearate-co-ε-caprolactone) (PGC-C18)	7.2–7.7 μm	Camptothecin-11(CPT-11) and 7-ethyl-10-hydroxycamptothecin (SN-38)	99 %	Diffusion	90 days	Human colorectal cancer HT-29 cells	[27]
Poly-$_{L}$-lactide	1033±450 nm	5-fluorouracil (5-FU)	1.6–12.8 wt%	Diffusion	240 h	Human colorectal cancer HCT-116 cells	[28]
Poly(L-lactic acid)	1.52–2.52μm	Titanocene dichloride	4.0–9.7 wt %	Degradation of the polymeric matrix	184 h	Human lung cancer spc-a-1 cells	[29]
Poly(ε-caprolactone) (PCL)/gelatin (GT)	607.4–536.6 nm	7-ethyl-10-hydroxy camptothecin (SN-38)	86.5–91.8 %	Diffusion and anomalous transport	6 weeks	Human glioblastoma 251 and U87 cells	[30]
Poly(D,L-lactide-co-glycolide)/ polyethylene oxide (PLGA/PEO)	200±79 nm	Ferulic acid	N/A	Diffusion and degradation of polymeric matrix	240 h	Human breast carcinoma MCF-7 cells	[31]
Poly(L-lactide-co-D,L-lactide) (coPLA)/quaternized chitosan (QCh)	310±50 nm	Doxorubicin (DOX)	96.0 %	N/A	72 h	Human breast carcinoma MCF-7 cells	[32]
Polylactide (PLA)	300 nm	5-fluorouracil and oxaliplatin	4 and 20 wt%	Diffusion	48 h	Human colorectal cancer HCT-8 cells and mouse colorectal cancer CT-26 cells	[33]
Poly(ethylene glycol)–poly($_{L}$-lactic acid) (PEG–PLLA)	690–1350nm	1,3-bis(2-chloroethyl)-1-nitrosourea (BCNU)	5–30 wt%	Diffusion	72 h	Rat glioma C6 cells	[19]
Polyvinyl alcohol (PVA)/Chitoson (CS)	98–154 nm	Curcumin	N/A	Diffusion and degradation of polymeric matrix	10 days	Human breast MCF-7 cancer cells, Human liver carcinoma HepG2 cells	[34]
Poly-($_{D,L}$-lactide-*co*-glycolide) (PLGA)	930 nm-3.5μm	Paclitaxel	94–98 %	Degradation of polymeric matrix	80 days	Rat C6 glioma cells	[35]
Poly($_{L}$-actide) (PLA) / poly($_{D,L}$-lactide-*co*-glucolic acid) (PLGA)	0.4–1.7μm	Cisplatin	90 %	Diffusion	75 days	Rat C6 glioma cells	[36]
Poly(ε-caprolactone) (PCL)	500±20 nm	Camptothecin	59 %	Diffusion	144 h	Mouse myoblast C2C12 cells	[37]
Polycaprolactone (PCL)/silk fibroin (SF)	281–315 nm	Titanocene dichloride	0.01–0.03 wt%	The degradation of the matrix	6 days	Human breast cancer MCF-7 cells	[38]
PCL	286±90 nm	Curcumin, aloe vera, neem extract	77–91 %	N/A	25 days	Human breast cancer MCF-7cells and lung cancer A459 cells	[39]
Poly ($_{D,L}$-lactic-co-glycolic) acid (PLGA)	160±10 nm	Curcumin	66–81 %	Diffusion and erosion	264 h	Skin cancer A431 cells	[40]
Poly(ethylene glycol)-*b*-poly($_{L}$-lactic acid) PEG-PLA	750 nm	DOX	N/A	Diffusion and degradation of fiber matrix	12 h	Human hepatocarcinoma SMMC-7721cells	[41]
Poly($_{L}$-lactide-co-$_{D,L}$-lactide) (coPLA)	580–640 nm	DOX	3 and 6 wt%	Diffusion	~210 min	Human cervical cancer HeLa cells	[42]
Quaternized chitosan (QCh)/coPLA	310–470 nm	DOX	3 and 6 wt%	Diffusion	~210 min	Human cervical cancer HeLa cells	[42]
Poly(ε-caprolactone) (PCL) and gelatin (GEL)	260–310 nm	Piperine	10–30 wt%	Hydrolytic degradation of PCL	5 days	Human cervical cancer HeLa cells and human breast MCF-7 cancer cells	[43]
Polyvinyl pyrrolidone (PVP)	485±123 nm	Curcumin	10 wt%	Dissolution	48 h	Murine melanoma B16 cells	[44]

Delivery systems	Fiber diameter	Drug	Drug loading efficiency or content	Drug release mechanism	Drug release time	Cancer types	Ref
Collagen/poly(N-isopropyl acrylamide)/chitosan	300–650 nm	5-fluorouracil	N/A	Dissolution	72 h	Human cervical cancer HeLa cells, human osteosarcoma MG-63 cells, and human breast carcinoma cells MCF-7 cell	[45]
Polylactide (PLLA)	0.4–1.3μm	DOX	3 and 6 wt%	Diffusion and hydrolysis and degradation of PLLA	N/A	Secondary hepatic carcinoma SHCC cells	[46]
Polylactide (PLA)	200–850 nm	Sodium dichloroacetate (DCA) and diisopropylamine dichloroacetate (DADA)	N/A	N/A	15 days (in vivo)	Colorectal cancer C26 cells	[47]
Polylactide (PLA)	N/A	Dichloroacetate	35 wt%	N/A	N/A	Murine cervical cancer U14 cells	[48]
Chitosan (CS)/ polyethylene oxide (PEO)	300nm	Paclitaxel	N/A	Diffusion	200 h	Prostate cancer DU145 cells	[49]
Poly(lacticco-glycolic acid) (PLGA)	262±33nm	Daunorubicin	N/A	Diffusion and the polymer nanofiber degradation	51 days	Human epidermoid carcinoma A431 cells	[50]
Polycaprolactone (PCL)	739±77 nm (PCL/EGCG), 647±55 nm (PCL/CA)	(−)-epigallocatechin-3-O-gallate (EGCG) and caffeic acid (CA)	1.1 wt%	Diffusion and the degradation of PCL	9 days	Human gastric cancer MKN28 cells	[51]
Poly-$_{D,L}$-lactide (PDLLA)	0.4–12.6 μm	Docetaxel	5–20 wt%	N/A	24 days	Mouse breast cancer 4T1 cells	[52]
Poly (L-lactic acid) (PLA)	200–1900 nm	Cisplatin	80.12–94.60%	Diffusion and degradation of PLLA matrix	280 h	Human lung cancer Apc-a-1 cells	[53]
Poly($_{DL}$-lactic acid)–poly(ethylene glycol) (PELA)	780±50 nm	Hydroxycamptothecin (HCPT)	92%−96%	Diffusion and the degradation of polymeric matrix	20 days	Human breast cancer MCF-7 cells	[54]
Poly(N-isopropylacrylamide-co-acrylamide-co-vinylpyrrolidone) P(NIPAAM-AAm-VP)	175.90 nm	DOX	10–50 wt%	Diffusion	30 days	Human lung cancer A549 cells	[55]
Poly(ethylene oxide)/polylactide	200–500 nm	Cisplatin	N/A	Diffusion and frame erosion	24 h	Murine cervical cancer U14cells	[56]
Poly(ethylene glycol)-poly(L-lactic acid) (PEG–PLA)	730 nm	Paclitaxel and doxorubicin hydrochloride	97.0% and 90.6%	Diffusion	35 h	Murine glioma C6 cells	[57]
Poly(L-lactide) (PLA)	200–300 nm	Oxaliplatin and cyclophosphamide	10 and 7.5 wt %	Diffusion	24 h	Human hepatocellular cancer HCC cells	[58]

Table 2.

Core-shell structured nanofibers for anticancer drug delivery.

Shell	Core	Fiber diameter	Drug	Drug loading efficiency or content	Drug release mechanism	Drug release time	Cancer types	Ref
Glutaraldehyde (GA) vapor crosslinked chitosan (CS)	Polyvinyl alcohol (PVA)	235–280 nm	DOX	N/A	Degradation of matrix	120 h	Human ovarian cancer SKOV3 cells	[61]
Genipin cross-linked gelatin	DOX-encapsulated folate (FA)-conjugated PCL-PEG copolymer	211.20±39.89 nm	DOX	71.08 %	N/A	~700 h	Mouse breast cancer 4T1 cells	[62]
PVA	$Pt_{(IV)}$ prodrug-backboned micelle and dichloroacetate (DCA)	470±89 nm	$Pt_{(IV)}$ prodrug and dichloroacetate (DCA)	0.55 % and 18.03 %	Diffusion	72 h	Human cervical cancer HeLa cells	[64]
PCL, PIPAAm copolymerized with acrylic acid (AAc)	DOX encapsulated poly-ethylene oxide (PEO)	274–318 nm	DOX	1.67 wt%	Diffusion	135 min	Mouse breast cancer 4T1 cells	[66]
Poly (N-isopropylacrylamide) (PNIPAM)	Silica-coated gold nanorods (Au@SiO_2-DOX) and polyhedral oligomeric silsesquinoxanes (POSS)	838±164 nm	DOX	N/A	Diffusion	~250 min	Human cervical cancer HeLa cells	[67]
Chitosan/poly(lactic acid) (PLA)	Graphene oxide/TiO_2/doxorubicin (GO/TiO_2/DOX) composite	210 nm	DOX	92–97 %	Diffusion and degradation of polymeric matrix	14 days	Human lung cancer A549 cells	[70]
Poly (lactic acid) (PLA)	Daunorubicin loaded carboxylated multiwalled carbon nanotube (MWCNT)/Fe_3O_4 composite	95 nm	Daunorubicin	93–97 %	Diffusion and relaxation	15 days	Human leukemia cancer K562 cells	[71]
Poly(e-caprolactone) (PCL)	Green tea polyphenol (GTP)-attached MWCNT	200–400 nm	Green tea polyphenol (GTP)	5 and 10 wt %	Diffusion and degradation of polymeric matrix	7 days	Human lung cancer A549 cells and human liver carcinoma HepG-2 cells	[72]
Polylactic acid (PLA)/polyethylene glycol (PEG)	MWCNT and DOX	225 nm	DOX	87–94 %	Diffusion	60 days	Human lung cancer A549 cells	[73]
Polyethylene oxide (PEO)/chitosan (CS)	GO and DOX	85 nm	DOX	98 %-	pH dependent diffusion	60 days	Human lung adenocarcinoma A549 cells	[74]
Poly(lactic-co-glycolic acid) (PLGA)	DOX@ mesoporous silica nanoparticles (DOX@MSNs) and hydroxycamptothecin @hydroxyapatite nanoparticles (CPT @HANPs)	857 nm	DOX and hydroxycamptothecin	0.045 and 0.08 wt%	PLGA swelling and chain relaxation	288 h	Human cervical cancer HeLa cells	[75]

Shell	Core	Fiber diameter	Drug	Drug loading efficiency or content	Drug release mechanism	Drug release time	Cancer types	Ref
Polylactic (PLA)	Naturel pearl powder, and DOX	400–500 nm	DOX	N/A	Degradation of matrix	25 days	Human cervical cancer HeLa cells	[76]
Poly (ε-caprolactone) (PCL)	Poly (ε-caprolactone) (PCL)/ mycophenolic acid (MPA)	1.7 μm	Mycophenolic acid (MPA)	95 %	N/A	96 h	Human glioblastoma multiforme U-87 MG cells	[77]
Poly($_L$-lactic acid-co-ε-caprolactone) (75:25) (P(LLA-CL)	Paclitaxel	233–1459 nm	Paclitaxel	> 80 %	Diffusion, the erosion and swelling of the polymer matrix, the drgradation of polymer and paclitaxel dissolution/partitioning	60 days	Human cervical cancer HeLa cells	[78]
Poly (ε-caprolactone diol) based polyurethane (PCL-Diol-b-PU)	Temozolomide (TMZ) loaded chitosan (CS) nanoparticles	235 nm	Temozolomide (TMZ)	92.8±0.2 %	Diffusion	30 days	Human glioblastoma U-87 MG cells	[79]
Poly (ε-caprolactone diol) based polyurethane (PCL-Diol-b-PU)	Au nanoparticles and temozolomide (TMZ)	270 nm	Temozolomide (TMZ)	93.8–94.2 %	Diffusion	30 days	Human glioblastoma U-87 MG cells	[80]
Poly($_L$-lactide) (PLLA)	Fullerene C_{70} and paclitaxel	350–750 nm	Paclitaxel	5 wt%	Diffusion	72 h	Human liver carcinoma HepG-2 cells	[81]
Poly(dl-lactic acid)-poly(ethylene glycol) (PELA)	2-Hydroxypropyl--cyclodextrin (HPCD) and hydroxycamptothecin	540±70 nm	Hydroxycamptothecin	> 95 %	Diffusion	20 days	Human hepatocellular carcinoma HepG2 cells	[82]
Polylactide (PLA)	Fe_3O_4 nanoparticles	100 nm	Daunorubicin	N/A	External magnetic field-assisted diffusion	N/A	Human leukemia K562 cells	[83]
Poly($_L$-lactic acid) (PLLA)	DOX loaded mesoporous silica nanoparticles (MSNs)	585–1439 nm	DOX	N/A	N/A	20 days	Human cervical cancer HeLa cells	[84]
Polysulphone (PSu)	Nanohydroxyapatite (nHA)	300–700 nm	5-FU	5 and 10 wt %	Diffusion	250 h	Human cervical cancer HeLa cells, human osteosarcoma MG-63 cells and human breast cancer MCF-7 cells	[85]
Poly(lactic-co-glycolic acid)/gelatin (PLGA/GE)	DOX-loaded mesoporous ZnO (DOX@mZnO) and camptothecin	284.7 nm	DOX and camptothecin	N/A	N/A	~170 h	Human liver carcinoma HepG2 cells	[86]
Polyvinyl alcohol (PVA)	Curcumin encapsulated mPEG-PCL micelles and DOX	220–314 nm	Curcumin and DOX	67.76 %	Diffusion and the de-assembly of micelles	14 days	Human cervical cancer HeLa cells	[87]
Poly(Lactic-Co-Glycolic Acid)	DOX-loaded carbon nanotubes	528.5–1058.8 nm	DOX	81.5 %	Diffusion	~16 days	Human cervical cancer HeLa cells	[88]

Shell	Core	Fiber diameter	Drug	Drug loading efficiency or content	Drug release mechanism	Drug release time	Cancer types	Ref
Poly($_L$-lactic acid) (PLLA)	DOX-loaded mesoporous silica (MSN/DOX) and DOX	780 nm	DOX	N/A	Diffusion	120 days	Human breast cancer MDA-MB-231 cells	[89]
Poly ($_L$-lactide) (PLLA)	DOX/sodium bicarbonate (SB) loaded MSNs	800 nm	DOX	N/A	Diffusion	100 days	Human breast cancer MDA-MB-231 cells	[90]
Poly(lactic-co-glycolic acid) (PLGA)	DOX loaded n-HA	577±133 nm	DOX	N/A	Diffusion	30 days	Human epithelial carcinoma kB cell	[91]
Poly(lactic-co-glycolic acid)/chitosan (PLGA/CS)	DOX loaded SiO_2 nanoparticles (DOX@SiO_2)	744 nm	DOX	N/A	Diffusion	369 h	Human cervical cancer HeLa cells	[92]

Small. Author manuscript; available in PMC 2019 December 27.

Table 3.

Summary of advantages and challenges of LDDSs for solo cancer therapy.

	Advantages	Challenges
LDDS for chemotherapy	✓ Maintaining the on-site dose at relatively high concentration ✓ Avoid excessive drug circulation ✓ Prolonged drug release ✓ Feasibility for delivering insoluble drugs and peptides with short half-life time.	■ Prolonged drug release induces the strong resistance of cancer cells against chemotherapeutics, known as multiple drug resistance (MDR). ■ Inevitable side effect at certain degree
LDDS for photothermal therapy (PTT)	✓ Thermal ablation with high efficiency ✓ Tissue penetration ✓ Feasibility ✓ Non-intrusive ✓ Remote control ✓ Oxygen independence	■ Inhomogeneous heat distribution within tumor tissues ■ Limited penetration for deep-located tumors ■ Inflammation induced by hyperthermia ■ Damage to healthy tissue ■ Upregulating the expression of heat shock protein (HSP)
LDDS for magnetic thermal therapy (MHT)	✓ Thermal ablation with high efficiency ✓ Superior tissue penetration enabling cancer treatment at high depth ✓ Remote control ✓ Feasibility ✓ Non-intrusive ✓ Remote control ✓ Oxygen independence	■ Inhomogeneous heat distribution within tumor tissues ■ Damage to healthy tissue ■ Heat resistance
LDDS for photodynamic therapy (PDT)	✓ Non-intrusive ✓ Minimal damage to normal tissue ✓ Low dark toxicity ✓ No drug resistance ✓ Repeated treatment	■ Oxygen dependence. ■ Limited penetration of excitation light (UV or visible light) for treating deep-seated tumors. ■ Short lifetime of singlet oxygen generated ■ Low diffusion distance of singlet oxygen
LDDS for gene therapy	✓ Relatively high content of therapeutic genes at the tumor site ✓ Maintaining gene activity ✓ Low systematic toxicity	■ Poor capability in intracellular delivery of therapeutic genes ■ Low gene silencing effect ■ Safety concern